

Diffusion-based Semi-supervised Spectral Algorithm for Regression on Manifolds [†]

Weichun Xia, Jiaxin Jiang, and Lei Shi

School of Mathematical Sciences and Shanghai Key Laboratory for Contemporary Applied Mathematics, Fudan University, Shanghai, 200433, China.

Abstract

We introduce a novel diffusion-based spectral algorithm to tackle regression analysis on high-dimensional data, particularly data embedded within lower-dimensional manifolds. Traditional spectral algorithms often fall short in such contexts, primarily due to the reliance on predetermined kernel functions, which inadequately address the complex structures inherent in manifold-based data. By employing graph Laplacian approximation, our method uses the local estimation property of heat kernel, offering an adaptive, data-driven approach to overcome this obstacle. Another distinct advantage of our algorithm lies in its semi-supervised learning framework, enabling it to fully use the additional unlabeled data. This ability enhances the performance by allowing the algorithm to dig the spectrum and curvature of the data manifold, providing a more comprehensive understanding of the dataset. Moreover, our algorithm performs in an entirely data-driven manner, operating directly within the intrinsic manifold structure of the data, without requiring any predefined manifold information. We provide a convergence analysis of our algorithm. Our findings reveal that the algorithm achieves a convergence rate that depends solely on the intrinsic dimension of the underlying manifold, thereby avoiding the curse of dimensionality associated with the higher ambient dimension.

Keywords: Manifold learning, Heat kernel, Graph Laplacian, High-dimensional approximation, Semi-supervised learning, Convergence analysis

1 Introduction

High-dimensional data are increasingly prevalent across various fields within modern machine learning, presenting unique challenges. Specifically, the obstacle people often encounter is the small sample size compared to the high dimensionality of data and the “curse of dimensionality”, a concept introduced by [3], resulting in poor performance. This complex data structure necessitates novel approaches and theoretical proceedings in statistical analysis and inference. Recent literature [26, 13, 17] has illuminated that, in many instances, the practical input data tends to reside within a lower-dimensional, nonlinear manifold. This suggests that the input

[†] The work described in this paper is supported by the National Natural Science Foundation of China (Grants No.12171039) and Shanghai Science and Technology Program [Project No. 21JC1400600]. Email addresses: 22210180107@m.fudan.edu.cn (W. Xia), jxjiang20@fudan.edu.cn (J. Jiang), leishi@fudan.edu.cn (L. Shi). The corresponding author is Lei Shi.

data space X , can be conceptualized as a compact and connected Riemannian manifold \mathcal{M} embedding into ambient Euclidean space \mathbb{R}^D , where the manifold dimension d is substantially less than D . This notion is in harmony with the widely acknowledged low-dimensional manifold hypothesis, which has gained significant attention in contemporary research, e.g. [8, 30, 34]. This geometric perspective paves the way for addressing the intrinsic complexities posed by high-dimensional data.

In the domain of data analysis and pattern recognition, regression emerges as a fundamental problem discerning relationships between input (explanatory) and output (response) variables. In this paper, we primarily study the non-parametric regression problem (1.1). The input variable x originates from a lower-dimensional manifold \mathcal{M} , the output variable $y \in \mathbb{R}$ is real, and they are governed by an unknown distribution \mathcal{P} over the product space $\mathcal{M} \times \mathbb{R}$. Given a dataset $D = \{(x_i, y_i)\}_{i=1}^n$ that is independently and identically distributed according to \mathcal{P} , our goal is to identify or approximate the optimal estimator $f^* : \mathcal{M} \rightarrow \mathbb{R}$ that minimizes the mean-squared error, in a specified function space \mathcal{F} , e.g. the space of measurable functions:

$$f^* = \arg \min_{f \in \mathcal{F}} \int_{\mathcal{M} \times \mathbb{R}} (y - f(x))^2 d\mathcal{P}(x, y). \quad (1.1)$$

Referencing the classical literature [33], with the knowledge of \mathcal{P} , an explicit calculation finds the optimal regression function f^* in the whole measurable space as

$$f^*(x) = \int_{\mathbb{R}} y d\mathcal{P}(y|x),$$

where $\mathcal{P}(\cdot|x)$ denotes the conditional distribution of \mathcal{P} over \mathbb{R} given x .

The regression problem (1.1) has been extensively explored, leading to diverse methodologies. For an in-depth exploration, one can refer to comprehensive monographs [19, 33]. Among the numerous strategies, spectral algorithms, as suggested by [1], stand out due to their effective implementation, which involves applying a filter function to the spectra of a finite-dimensional kernel matrix. The efficacy of these algorithms is largely ascribed to the regularization achieved via a carefully selected set of filter functions. Moreover, the rich choice of regularization function allows spectral algorithms to conclude a broad range of popular regression algorithms, which is specified in Subsection 2.3. This adaptability is particularly noteworthy, emphasizing the significance of spectral algorithms in regression analysis. By leveraging the strengths of different regularization strategies, spectral algorithms offer an important framework for tackling complex regression problems. For more detailed analyses and discussions of spectral algorithms, we refer to recent studies such as [5, 43, 14].

Although the spectral algorithm has gained widespread application, its efficacy is occasionally hampered by several issues, among which the selection of the kernel function stands out as a particularly daunting challenge. As detailed in Subsection 2.3, the computation of the spectral algorithm estimator is fundamentally dependent on the kernel matrix $(K(x_i, x_j))_{i,j=1}^n$, where $K(x, x')$ is the kernel function defined over the input manifold. Traditional approaches often employ kernels such as radial basis kernels and polynomial kernels, which we refer to [53, 55] for more details. Nevertheless, these conventional kernels tend to underperform in scenarios involving manifold input data, primarily because they overlook the intrinsic structure of data. To address the complexities presented by the manifold structure of data, recent studies have shifted towards utilizing manifold-based bandlimited kernels and heat kernels, as seen in [44, 62]. These kernels are designed with the input manifold's intrinsic structure

in mind, notably leveraging the spectrum of the Laplace-Beltrami operator and curvatures of the data manifold. This focus on the manifold’s inherent features allows for remarkable theoretical convergence properties, characterized by a rapid convergence rate that depends solely on the manifold’s dimension d , and remains unaffected by the higher ambient dimension D . This presents a substantial improvement over traditional kernels, which often suffer from the curse of dimensionality. The theoretical benefits, including the enhanced convergence rate, of these manifold-based kernels, have also been validated in [44, 62], highlighting their efficiency in advancing the spectral algorithm’s applicability in high-dimensional data analysis.

While manifold-based kernels offer theoretical advantages, their practical application is hindered by the challenge of calculating these functions, which is requisite in the algorithms. Our work is inspired by graph Laplacian methods, well-regarded in the literature of manifold learning (see e.g. [2, 18, 59, 45]) for their effectiveness in capturing the local geometric and topological structures of input manifolds. We adopt these methods to estimate the manifold heat kernel, introducing a data-driven, adaptive kernel matrix as an alternative to the difficult-to-calculate manifold-based kernel matrix. This approach not only effectively and efficiently overcomes the implementation hurdle but also preserves the superior qualities of manifold-based kernels by leveraging the local approximation property of the heat kernel on data manifold. To our knowledge, the specific application of graph Laplacian approximation for manifold heat kernel estimation is still relatively uncharted, with few literature venturing into this domain [23, 24]. Our paper integrates this estimation method with spectral algorithms to introduce a novel diffusion-based spectral algorithm. See Algorithm 1. This development expands the capabilities of spectral algorithms in processing complex manifold data structures.

One of the superiorities of our algorithm is its semi-supervised learning nature. In traditional supervised learning scenarios, labeling data necessitates considerable effort, such as transcribing for speech recognition tasks, or might require specialized expertise, like determining the health status of a brain scan. Conversely, in many fields, including computer vision, natural language processing, and speech recognition, acquiring unlabeled data is often much easier and can be done on a larger scale with less effort. Carrying out the principles of classical semi-supervised learning, our algorithm enables the use of additional unlabeled manifold samples. These samples inherently reflect the geometric and topological structure of the input manifold, bearing a potential enhancement in the performance of the spectral algorithm beyond what is achievable with solely labeled data. This ability to use both labeled and unlabeled data for improving learning outcomes presents a substantial enhancement over traditional spectral algorithms, which rely exclusively on labeled data. Additionally, unlike methods that pre-process data through dimension reduction to simplify regression tasks, our algorithm tackles the complexity head-on by operating directly within the intrinsic manifold structure of data. This approach offers a direct solution to the intricate problem of regression on manifolds, requiring no predefined manifold information. Our algorithm operates entirely on the available data, sticking to a fully data-driven methodology. These characteristics showcase our algorithm’s capability to navigate the manifold’s inherent complexities efficiently and effectively.

In this paper, we further provide a rigorous convergence rate analysis of our novel algorithm. Detailed theoretical results are elaborated in Subsection 3.2. Drawing from our main Theorem 4, we demonstrate that, for a selection of filter functions commonly used in traditional spectral algorithms, including kernel ridge regression and kernel principal component

regression, our diffusion-based spectral algorithm achieves a convergence rate of

$$\sup_{1 \leq j \leq N} |\tilde{f}_{D,\lambda}(j) - f^*(x_j)| = \tilde{O} \left(m^{-\frac{1}{2} + \alpha} + m^{\frac{3}{2r+1} + 1} \left(\frac{1}{K} + \left(\frac{\log N}{N} \right)^{\frac{1}{2d+8}} \right) \right).$$

In this expression, the notation $\tilde{O}(\cdot)$ omits lower-order terms compared to the primary term. The symbol $\tilde{f}_{D,\lambda}$ denotes the estimator derived from our diffusion-based spectral algorithm, m represents the number of labeled inputs, N signifies the total number of inputs (both labeled and unlabeled), $m \ll K < N$ refers to a truncation hyperparameter introduced in subsection 2.4, $r > 1$ is a constant introduced in Assumption 1, and $0 < \alpha < 1/2$ can be chosen arbitrarily small. This pointwise convergence rate is applicable across all $1 \leq j \leq N$, particularly within the unlabeled dataset, which is solely dependent on the intrinsic dimension d of the input manifold, irrespective of the considerably higher ambient dimension D . This property reflects the benefits observed in classical spectral algorithms that employ manifold-based bandlimited kernels or heat kernels, further demonstrating the effectiveness and efficiency of our algorithm in dealing with high-dimensional data through a semi-supervised learning framework.

The remainder of this paper is organized as follows. In Section 2, we introduce key concepts and notations in our paper. In Section 3, we present the diffusion-based spectral algorithm with a comprehensive convergence analysis. In Section 4, we illustrate the validity of the algorithm through numerical experiments. In Section 5, we rigorously prove our main theoretical theorem. We provide additional details and analyses that complement the main text in the Appendix.

2 Notations and Theoretical Backgrounds

Before delving into a detailed discussion, we introduce several notations. As mentioned in Section 1, our input data space is defined as a Riemannian manifold \mathcal{M} with dimension d , and the output space as the real line \mathbb{R} . We consider an unknown distribution \mathcal{P} on the product space $\mathcal{M} \times \mathbb{R}$, denoting its marginal distribution on \mathcal{M} as ν , and the conditional distribution given $x \in \mathcal{M}$ on \mathbb{R} as $\mathcal{P}(\cdot|x)$. Furthermore, we assume this marginal distribution ν to be uniform, which means that it differs from the Riemannian volume measure μ_g (defined in (2.1) below) only by a constant factor $p = \frac{1}{\text{vol}\mathcal{M}}$. For simplicity, in subsequent discussions, we will use the notation $L^2(\mu_g)$ and $L^2(\nu)$ to refer to the L^2 -space with respect to the Riemannian volume measure μ_g and the uniform measure ν on \mathcal{M} respectively.

2.1 Manifold and Heat Kernel

In this subsection, we introduce the concepts of Riemannian manifolds and the heat kernel. We consider a compact, connected Riemannian manifold \mathcal{M} of dimension d , embedded into a higher-dimensional ambient Euclidean space \mathbb{R}^D , where $d \ll D$. The fundamental geometry of this manifold, the Riemannian metric g and the Levi-Civita connection ∇ , are derived from the manifold's embedding in \mathbb{R}^D . The Riemannian metric g gives rise to a unique Radon measure μ_g on \mathcal{M} , commonly referred to as the Riemannian volume measure. This measure is defined as

$$\int_{\mathcal{M}} f d\mu_g = \sum_j \int_{\varphi_j(U_j)} \left(\psi_j f \sqrt{\det(g_{ij})} \right) \circ \varphi_j^{-1} dx, \quad (2.1)$$

where dx denotes the Lebesgue measure on \mathbb{R}^d , $\{U_j, \varphi_j\}$ represents a smooth atlas of \mathcal{M} , and $\{\psi_j\}$ signifies the partition of unity subordinate to the atlas covering $\{U_j\}$. If \mathcal{M} is additionally orientable, we can locally define a smooth, non-zero volume form on \mathcal{M} as $\omega = \sqrt{\det(g_{ij})} dx^1 \wedge \dots \wedge dx^m$, given a positively oriented orthonormal basis of $T_u(\mathcal{M})$. This allows the Riemannian volume measure μ_g to be elegantly represented as $\int_{\mathcal{M}} f d\mu_g = \int_{\mathcal{M}} f \omega$. For a more thorough exploration of integration on Riemannian manifolds, one may refer to standard literature such as [15, 52, 47].

We introduce the Laplace-Beltrami operator on a Riemannian manifold \mathcal{M} . It is often abbreviated as the Laplacian, a concept fundamental to the study of differential geometry with applications in manifold learning. This operator is determined by the Levi-Civita connection ∇ and its Riemannian metric g , as detailed in the textbooks [47, 40]. For any smooth function $f \in C^\infty(\mathcal{M})$, the Laplacian Δf is defined as the negative divergence of the gradient vector field of f ,

$$\Delta f = -\operatorname{div}(\nabla f).$$

And in local coordinates, this operator has an explicit expression as

$$\Delta f = -\frac{1}{\sqrt{\det g}} \partial_i \left(g^{ij} \sqrt{\det g} \partial_j f \right),$$

where we have adopted the Einstein summation convention. Choosing a negative sign in definition ensures that the Laplacian remains a positive operator, aligning with the conventions of mathematical physics and differential geometry. For the classical case where the manifold \mathcal{M} is the Euclidean space \mathbb{R}^d , the Laplacian corresponds to the familiar second-order derivative operator $-\sum_{i=1}^d \partial_i^2$. Initially, the Laplacian acts as a self-adjoint, positive, and semi-definite operator on the space of smooth functions defined on \mathcal{M} . However, it can be uniquely extended to a self-adjoint, positive, and semi-definite operator on the space $L^2(\mu_g)$ through Friedrich's extension theorem, a process thoroughly examined in the analytical studies by [57, 50]. This extension of the Laplacian preserves its fundamental properties and enables a broader application in the analysis of functions on Riemannian manifold, and we also refer to it as Laplacian.

Consider the heat equation on a Riemannian manifold \mathcal{M} , formulated as:

$$\begin{cases} \frac{\partial u}{\partial t} + \Delta u = 0, & t > 0 \\ u|_{t=0} = f \end{cases}$$

with a smooth function $f : \mathcal{M} \rightarrow \mathbb{R}$. Given that \mathcal{M} is both smooth and compact, this equation guarantees a unique smooth solution $u = e^{-t\Delta} f$. Drawing on classical literature such as [20, 29], for the heat semi-group $e^{-t\Delta}$, there exists a unique function $H : \mathcal{M} \times \mathcal{M} \times (0, \infty) \rightarrow \mathbb{R}$ such that:

$$(e^{-t\Delta} f)(u) = \int_{\mathcal{M}} H(u, u', t) f(u') d\mu_g(u'). \quad (2.2)$$

Here, $H_t(u, u') = H(u, u', t)$ is called the heat kernel, characterized by its diffusion time t . Specifically, for $\mathcal{M} = \mathbb{R}^d$, H_t reduces to the well-known Gaussian kernel $H_t(x, x') = e^{-\frac{|x-x'|^2}{4t}} / (4\pi t)^{\frac{d}{2}}$. Gaussian-type functions could be used to approximate the manifold heat kernel, especially for closely positioned u, u' and small t , exhibiting an approximation error

$$\left| H_t(u, u') - \frac{1}{(4\pi t)^{\frac{d}{2}}} e^{-\frac{d_{\mathcal{M}}(u, u')^2}{4t}} (u_0 + tu_1) \right| \leq O(t), \quad (2.3)$$

where u_0, u_1 are smooth functions locally close to 1, and $d_{\mathcal{M}}(u, u')$ denotes the geodesic distance between u and u' on \mathcal{M} . This local approximation property is crucial for estimating the Laplacian's eigensystem using graph Laplacian techniques, which will be further explored in Subsection 2.4. A classical assumption about the heat kernel is its boundedness, namely

$$\sup_{u \in \mathcal{M}} H_t(u, u) \leq \kappa^2 \quad (2.4)$$

with some constant $\kappa \geq 1$. Given the compactness of \mathcal{M} and inherently bounded sectional curvature and Ricci curvature, this boundedness condition is naturally satisfied by the heat kernel comparison theorem. Further details can be found in [37].

Given that the Laplacian Δ is a self-adjoint, positive, and semi-definite operator on $L^2(\mu_g)$, the celebrated Sturm-Liouville theorem enables us to identify an orthonormal basis $\{\psi_k\}_{k \in \mathbb{N}}$ for $L^2(\mu_g)$. Each ψ_k in this basis is smooth on \mathcal{M} and adheres to

$$\Delta \psi_k = \mu_k \psi_k \quad (2.5)$$

for all k . The sequence of eigenvalues

$$0 = \mu_1 \leq \mu_2 \leq \dots \leq \mu_k \rightarrow +\infty$$

corresponding to $\{\psi_k\}$, are aligned in an unbounded increase. The rate at which these eigenvalues grow directly relates to the manifold's dimension. This relationship is elaborated in the following Lemma 1. The following literature [36, 41, 15] offers a deeper exploration of these foundational results.

Lemma 1. *Suppose that \mathcal{M} is a compact, connected Riemannian manifold with dimension d . Then, for the eigensystem of Laplacian Δ on \mathcal{M} as in (2.5), for any $k \in \mathbb{N}$, we have the following estimations:*

$$C_{low} k^{\frac{2}{d}} \leq \mu_k \leq C_{up} k^{\frac{2}{d}}, \quad (2.6)$$

$$\|\psi_k\|_{L^\infty(\mathcal{M})} \leq D_1 \mu_k^{\frac{d-1}{4}}, \quad (2.7)$$

where C_{low} , C_{up} , and D_1 are absolute constants only rely on \mathcal{M} .

Building on the eigensystem of the Laplacian as previously discussed in (2.5), the heat semi-group $e^{-t\Delta}$ can be characterized through its eigen-decomposition:

$$e^{-t\Delta} \psi_k = e^{-t\mu_k} \psi_k. \quad (2.8)$$

This directly leads to the spectral decomposition of the heat kernel H_t , which, according to Mercer's theorem (see e.g. [60]), is expressed as

$$H_t(u, u') = \sum_{k=1}^{\infty} e^{-t\mu_k} \psi_k(u) \psi_k(u'), \quad (2.9)$$

ensuring a uniformly and absolutely convergent series.

2.2 Diffusion Space and Integral Operator

In this subsection, we clarify the concept of diffusion space on a Riemannian manifold \mathcal{M} and the related integral operators. Given any fix $t > 0$, the diffusion space, denoted as \mathcal{H}_t (with diffusion time t), is defined as

$$\mathcal{H}_t = e^{-\frac{t}{2}\Delta}L^2(\mu_g). \quad (2.10)$$

\mathcal{H}_t is structured as a Hilbert space equipped with an inner product

$$\langle f, g \rangle_{\mathcal{H}_t} = \langle e^{\frac{t}{2}\Delta}f, e^{\frac{t}{2}\Delta}g \rangle_{L^2(\mu_g)}. \quad (2.11)$$

Further, endowed with this inner product (2.11), \mathcal{H}_t constitutes a reproducing kernel Hilbert space (RKHS), with the heat kernel $H_t(u, u')$ serving as its reproducing kernel. This RKHS framework facilitates various significant attributes, as detailed in [22]. A key feature of the diffusion space is the embedding property:

$$\mathcal{H}_t \hookrightarrow \mathcal{H}_{t'} \hookrightarrow W^s(\mathcal{M}), \quad (2.12)$$

for all $0 < t' < t$ and $s > 0$, with $W^s(\mathcal{M})$ representing the s -order Sobolev space on \mathcal{M} under the $L^2(\mu_g)$ -norm. Given the compact embedding of the Sobolev space $W^s(\mathcal{M})$ into $C(\mathcal{M})$ for $s > \frac{d}{2}$, as noted by [35, 58], and considering the compactness of \mathcal{M} , it follows that any diffusion space \mathcal{H}_t can be compactly embedded into $L^\infty(\mathcal{M})$. Consequently, for any $t > 0$, there exists a constant A (dependent on t) such that

$$\|i : \mathcal{H}_t \hookrightarrow L^\infty\|_{op} \leq A,$$

where $\|\cdot\|_{op}$ denotes the operator norm. This embedding property, as explored in recent literature [25, 63, 62], plays a vital role in the convergence analysis.

Considering the inclusion map I_ν from \mathcal{H}_t to $L^2(\nu)$, we introduce its adjoint operator, I_ν^* , which is an integral operator mapping $L^2(\nu)$ back to \mathcal{H}_t :

$$(I_\nu^*f)(x) = \int_{\mathcal{M}} H_t(x, z)f(z)d\nu(z). \quad (2.13)$$

A straightforward examination reveals that both I_ν and I_ν^* qualify as Hilbert-Schmidt operators, hence they are inherently compact. The Hilbert-Schmidt norm of these operators meets the following relation

$$\|I_\nu^*\|_{\mathcal{L}^2(L^2(\nu), \mathcal{H}_t)} = \|I_\nu\|_{\mathcal{L}^2(\mathcal{H}_t, L^2(\nu))} = \|H_t\|_{L^2(\nu)} = \left(\int_{\mathcal{M}} H_t(x, x)d\nu(x) \right)^{\frac{1}{2}} \leq \kappa.$$

Further exploration of the integral operator I_ν^* involves composition with the inclusion map I_ν :

$$L_\nu = I_\nu I_\nu^* : L^2(\nu) \rightarrow L^2(\nu), \quad (2.14)$$

$$T_\nu = I_\nu^* I_\nu : \mathcal{H}_t \rightarrow \mathcal{H}_t. \quad (2.15)$$

The fact that these operators L_ν and T_ν are self-adjoint, positive-definite, and fall within the trace class, indicates that they are also Hilbert-Schmidt and compact by nature. The trace norm of these operators are

$$\|T_\nu\|_{\mathcal{L}^1(\mathcal{H}_t)} = \|L_\nu\|_{\mathcal{L}^1(L^2(\nu))} = \|I_\nu^*\|_{\mathcal{L}^2(L^2(\nu), \mathcal{H}_t)}^2 = \|I_\nu\|_{\mathcal{L}^2(\mathcal{H}_t, L^2(\nu))}^2.$$

In conclusion, L_ν represents the integral operator associated with the heat kernel H_t on $L^2(\nu)$, with respect to the uniform distribution ν . Let us compare it with the heat kernel integral operator on $L^2(\mu_g)$ with respect to the Riemannian volume measure μ_g , as in (2.2), which is the heat semi-group $e^{-t\Delta}$. Given that ν and μ_g differ only by a constant factor p , the eigen-decomposition of L_ν can be derived from (2.8) as

$$L_\nu \psi_k = p e^{-t\mu_k} \psi_k.$$

Given that $\{\psi_k\}_{k \in \mathbb{N}}$ constitutes an orthonormal basis of $L^2(\mu_g)$, it follows that $\{\varphi_k = p^{-\frac{1}{2}} \psi_k\}_{k \in \mathbb{N}}$ forms an orthonormal basis of $L^2(\nu)$. Furthermore, based on the inner product definition (2.11) on \mathcal{H}_t , $\{p^{\frac{1}{2}} e^{-\frac{t\mu_k}{2}} \varphi_k\}_{k \in \mathbb{N}}$ constitutes an orthonormal basis of \mathcal{H}_t . Since both L_ν and T_ν are self-adjoint and compact operators, the classical spectral theorem (see e.g. [50]) allows us to write down their spectral decompositions:

$$L_\nu = \sum_{k=1}^{\infty} p e^{-t\mu_k} \langle \cdot, \varphi_k \rangle_{L^2(\nu)} \varphi_k, \quad (2.16)$$

$$T_\nu = \sum_{k=1}^{\infty} p e^{-t\mu_k} \langle \cdot, p^{\frac{1}{2}} e^{-\frac{t\mu_k}{2}} \varphi_k \rangle_{\mathcal{H}_t} \cdot p^{\frac{1}{2}} e^{-\frac{t\mu_k}{2}} \varphi_k. \quad (2.17)$$

Additionally, the spectral decomposition for I_ν^* is given by:

$$I_\nu^* = \sum_{k=1}^{\infty} p^{\frac{1}{2}} e^{-\frac{t\mu_k}{2}} \langle \cdot, \varphi_k \rangle_{L^2(\nu)} \cdot p^{\frac{1}{2}} e^{-\frac{t\mu_k}{2}} \varphi_k. \quad (2.18)$$

Building on the integral operator L_ν , we explore the concept of α -power spaces within the diffusion space framework. These spaces, denoted as \mathcal{H}_t^α for any $\alpha > 0$, are defined as the range of a power of L_ν , i.e., $\mathcal{H}_t^\alpha = \text{Ran}(L_\nu^{\frac{\alpha}{2}})$. Leveraging the spectral decomposition of L_ν , we obtain an explicit representation for \mathcal{H}_t^α as

$$\mathcal{H}_t^\alpha = \left\{ \sum_{k=1}^{\infty} a_k p^{\frac{\alpha}{2}} e^{-\frac{\alpha\mu_k}{2}t} \varphi_k : \{a_k\}_{k=1}^{\infty} \in \ell^2(\mathbb{N}) \right\}. \quad (2.19)$$

Furthermore, \mathcal{H}_t^α is equipped with an α -power norm, defined as

$$\left\| \sum_{k=1}^{\infty} a_k p^{\frac{\alpha}{2}} e^{-\frac{\alpha\mu_k}{2}t} f_k \right\|_{\alpha} := \left\| \sum_{k=1}^{\infty} a_k p^{\frac{\alpha}{2}} e^{-\frac{\alpha\mu_k}{2}t} f_k \right\|_{\mathcal{H}_t^\alpha} = \|(a_k)\|_{\ell^2(\mathbb{N})} = \left(\sum_{k=1}^{\infty} a_k^2 \right)^{\frac{1}{2}}. \quad (2.20)$$

In discussions that follow, this α -power norm will be referred to using the notation $\|\cdot\|_{\alpha}$ for ease of reference. As a result of this formulation, we have

$$\left\| L_\nu^{\frac{\alpha}{2}}(f) \right\|_{\alpha} = \|f\|_{L^2(\nu)}.$$

This framework establishes that $L_\nu^{\frac{\alpha}{2}}$ acts as an isometry from $L^2(\nu)$ to \mathcal{H}_t^α , thereby confirming \mathcal{H}_t^α as a Hilbert space. This space is characterized by an orthonormal basis $\{p^{\frac{\alpha}{2}} e^{-\frac{\alpha\mu_k}{2}t} \varphi_k\}_{k \in \mathbb{N}}$. Notably, \mathcal{H}_t^α differs with $\mathcal{H}_{\alpha t}$ by a multiplication of $p^{\frac{1}{2}}$, and when $\alpha = 0$, it equals $L^2(\nu)$.

2.3 Regularization Family and Spectral Algorithm

In this subsection, we introduce the regularization family represented by different filter functions and its application in spectral algorithm estimators. Consider a labeled dataset $D^l = \{(x_i, y_i)\}_{i=1}^m$, independently and identically distributed from a distribution \mathcal{P} on $\mathcal{M} \times \mathbb{R}$. Our objective is to identify the optimal estimator $\hat{f} \in \mathcal{H}_t$ that minimizes the empirical risk

$$\hat{f} = \arg \min_{f \in \mathcal{H}_t} \frac{1}{m} \sum_{i=1}^m (y_i - f(x_i))^2. \quad (2.21)$$

The key to this regression problem is a finite rank sampling operator $H_{t,x}$, which maps y to $yH_t(x, \cdot)$ from \mathbb{R} to \mathcal{H}_t . The adjoint of this operator, $H_{t,x}^*$, is indeed the evaluation operator from \mathcal{H}_t to \mathbb{R} at a specific point $x \in \mathcal{M}$, defined as $H_{t,x}^* : f \mapsto f(x)$. Additionally, we introduce the sample covariance operator $T_\delta : \mathcal{H}_t \rightarrow \mathcal{H}_t$:

$$T_\delta = \frac{1}{m} \sum_{i=1}^m H_{t,x_i} H_{t,x_i}^*, \quad (2.22)$$

and define the sample basis function as

$$g_D = \frac{1}{m} \sum_{i=1}^m y_i H_t(x_i, \cdot) \in \mathcal{H}_t. \quad (2.23)$$

With these notions at hand, the regression problem (2.21) turns into the equation

$$T_\delta \hat{f} = g_D. \quad (2.24)$$

We refer to [60] for more details.

Due to the potential non-invertibility of the operator T_δ , we turn to a regularization approach to tackle problem (2.24). A set of functions, $\{g_\lambda : \mathbb{R}^+ \rightarrow \mathbb{R}^+\}_{\lambda>0}$, known as a regularization family or filter function, are defined to satisfy specific conditions

$$\begin{aligned} \sup_{0 < t \leq \kappa^2} |tg_\lambda(t)| &< 1, \\ \sup_{0 < t \leq \kappa^2} |1 - tg_\lambda(t)| &< 1, \\ \sup_{0 < t \leq \kappa^2} |g_\lambda(t)| &< \lambda^{-1}. \end{aligned} \quad (2.25)$$

These functions essentially aim to mimic the behavior of $t \rightarrow \frac{1}{t}$ while maintaining controlled behavior near zero. This approach ensures that they remain bounded by λ^{-1} , and effectively deal with the issue of non-invertibility in T_δ . For a chosen regularization family g_λ , we further define its qualification ξ , which indicates the adaptability of the regularization family, as the supremum of the following set:

$$\xi = \sup \left\{ \alpha > 0 : \sup_{0 < s \leq \kappa^2} |1 - sg_\lambda(s)| s^\alpha < \lambda^\alpha \right\}. \quad (2.26)$$

Leveraging the regularization family defined above, we propose the classical spectral algorithm estimator as a regularized solution to the regression problem (2.21) as

$$f_{D,\lambda} = g_\lambda(T_\delta)g_D. \quad (2.27)$$

In this setup, $g_\lambda(T_\delta)$ denotes the action of the function g_λ on T_δ through functional calculus, a concept elaborated in literature such as [49]. This methodology provides a feasible solution to the regression problem by circumventing the issue of non-invertibility and introduces a framework for applying spectral methods effectively in the context of empirical risk minimization.

Before delving deeper into the discussion of the spectral algorithm estimator, let us briefly illustrate a few examples. These instances serve as a primer to the broader and more detailed discussion in seminal works on the topic, including [51, 1, 28].

Example 1. (Kernel ridge regression) We choose the following regularization family

$$g_\lambda(t) = \frac{1}{\lambda + t},$$

which satisfies (2.26) with $\xi = 1$. In this situation, the spectral algorithm coincides with the kernel ridge regression (or Tikhonov regularization), which corresponds to the classical Hilbert-norm regularization of the original regression problem (2.21) as

$$f_{D,\lambda} = \arg \min_{f \in \mathcal{H}_t} \left\{ \frac{1}{m} \sum_{i=1}^m (y_i - f(x_i))^2 + \lambda \|f\|_{\mathcal{H}_t}^2 \right\}.$$

Example 2. (Kernel principal component regularization) We choose the following regularization family

$$g_\lambda(t) = \frac{1}{t} \mathbb{1}_{\{t \geq \lambda\}},$$

which satisfies (2.26) with $\xi = \infty$. In this situation, the spectral algorithm coincides with kernel principal component regularization (or spectral cut-off).

Example 3. (Gradient flow) We choose the following regularization family

$$g_\lambda(t) = \frac{1 - e^{-\frac{t}{\lambda}}}{t},$$

which satisfies (2.26) with $\xi = \infty$. In this situation, the spectral algorithm coincides with gradient flow.

It is noteworthy that the operator T_δ , as defined in (2.22), aligns with the integral operator defined in (2.15) about the empirical marginal distribution $\delta = \frac{1}{m} \sum_{i=1}^m \delta_{x_i}$ on \mathcal{M} . From this perspective we call T_δ the empirical integral operator. By definition, T_δ is inherently self-adjoint, positive semi-definite, and compact on \mathcal{H}_t . These properties facilitate an expression of T_δ 's eigensystem as

$$T_\delta \phi_k = \lambda_k \phi_k, \tag{2.28}$$

where the eigenvalues are organized in a non-increasing order $\lambda_1 \geq \dots \geq \lambda_m \geq \lambda_{m+1} = 0 = \dots$, with the fact that T_δ has a rank of at most m , and the eigenfunctions $\{\phi_k\}_{k \in \mathbb{N}}$ establish an orthonormal basis for \mathcal{H}_t . To further our understanding of the data set, we introduce the concept of the heat kernel matrix $H_t \in \mathbb{R}^{m \times m}$, characterized by:

$$H_t(i, j) \triangleq \frac{1}{m} H_t(x_i, x_j). \tag{2.29}$$

This matrix, comprised of heat kernel evaluations between data points, is crucial in the practical computation of spectral algorithm estimators. Given that the heat kernel matrix H_t is symmetric and positive-definite, it naturally supports an eigen-decomposition

$$H_t \hat{u}_k = \hat{\lambda}_k \hat{u}_k. \quad (2.30)$$

In this decomposition, eigenvalues are also organized in non-increasing order $\hat{\lambda}_1 \geq \dots \geq \hat{\lambda}_m > 0$, with the corresponding eigenvectors $\{\hat{u}_k\}_{k=1}^m$ forming an orthonormal basis of \mathbb{R}^m . The eigenvalues and eigenvectors of T_δ and H_t exhibit a close relationship, since the operator $H_{t,x_j}^* H_{t,x_i} : y \mapsto y H_t(x_i, x_j)$ from \mathbb{R} to \mathbb{R} has a matrix representation $H_t(x_i, x_j)$, whose matrix trace is scalar to T_δ . Specifically, we can explicitly express the relation between the eigensystem:

$$\begin{aligned} \lambda_k &= \hat{\lambda}_k \\ \phi_k &= \frac{1}{\sqrt{m \hat{\lambda}_k}} \sum_{i=1}^m \hat{u}_k(i) H_t(x_i, \cdot) \end{aligned} \quad (2.31)$$

with $\hat{u}_k(i)$ denoting the i -th entry of the eigenvector \hat{u}_k . Further insight into this connection is provided in [31]. Leveraging the eigen-decomposition of T_δ as in (2.28), the spectral algorithm estimator $f_{D,\lambda}$ can be unfolded as

$$f_{D,\lambda} = \sum_{k=1}^{\infty} g_\lambda(\lambda_k) \langle g_D, \phi_k \rangle_{\mathcal{H}_t} \cdot \phi_k. \quad (2.32)$$

This representation, informed by the relationship (2.31), is instrumental in the formulation and analysis of our algorithm.

2.4 Graph Laplacian and Heat Kernel Estimation

The representations of the spectral algorithm estimator $f_{D,\lambda}$, either through its definition (2.27) or its spectral decomposition (2.32), depend significantly on the explicit value of the heat kernel H_t on the data points. However, directly accessing or computing the heat kernel for a general manifold \mathcal{M} poses practical challenges. To address this obstacle, we turn to the graph Laplacian approximation, a powerful tool for approximating manifold structures using discrete data points.

Suppose that we are given a dataset $\{x_i\}_{i=1}^N$ independently and identically distributed from some distribution p on manifold \mathcal{M} . We may, for the sake of simplicity, consider p as the uniform distribution ν on \mathcal{M} . To analyze the manifold structure using this dataset, we construct a graph affinity matrix $W \in \mathbb{R}^{N \times N}$ and a diagonal degree matrix $D \in \mathbb{R}^{N \times N}$ with entries

$$\begin{aligned} W(i, j) &= K_\epsilon(x_i, x_j), \\ D(i, i) &= \sum_{j=1}^N W(i, j). \end{aligned} \quad (2.33)$$

Here, K_ϵ is defined as the Gaussian kernel

$$K_\epsilon(x, x') = \epsilon^{-\frac{d}{2}} \frac{1}{(4\pi)^{\frac{d}{2}}} \exp\left(-\frac{\|x - x'\|^2}{4\epsilon}\right),$$

where $\|\cdot\|$ denotes the usual Euclidean distance. This Gaussian kernel is selected for its ability to locally approximate the heat kernel, as exemplified in (2.3) for the Euclidean case, a property that could enhance the eigen-convergence rate of the graph Laplacian. Specifically, a recent studies [16] has revealed that such a local approximation result allows for an elaborate heat kernel interpolation method, thereby resulting in better convergence performance. The parameter $\epsilon > 0$ serves as a proxy for the diffusion time, which is also adopted in [54, 16]. It is worth noting that in other literature, such as [10, 24], the kernel parameters are expressed in terms of $\sqrt{\epsilon} > 0$, reflecting the local distance (or kernel bandwidth). Further, we define the un-normalized graph Laplacian $L_{un} \in \mathbb{R}^{N \times N}$ as

$$L_{un} = \frac{1}{p\epsilon N}(D - W). \quad (2.34)$$

This definition includes a constant normalization factor to ensure that L_{un} converges to the Laplacian Δ , and may not be involved in practical algorithms. The matrix L_{un} is characterized by its symmetry and positive semi-definiteness, with its smallest eigenvalue being zero. Moreover, as specified in Theorem 1, the eigensystem of L_{un} provides an effective approximation to that of Δ , demonstrating the utility of the graph Laplacian in approximating manifold structures from discrete data points. Detailed proofs of this theorem can be found in Appendix A. This approach bridges the gap between discrete data analysis and continuous manifold structures, offering a robust framework for understanding and exploring the intrinsic geometry of data manifolds. Recall that \mathcal{M} is a compact, connected Riemannian manifold with dimension d and ν is a uniform distribution on \mathcal{M} .

Theorem 1. *For any fixed $K \in \mathbb{N}$, assume that the eigenvalues μ_k of Δ are all of single multiplicity for every $k \leq K + 1$. Consider the first K eigenvalues $\{\tilde{\mu}_k\}_{k=1}^K$ and associated eigenvectors $\{\tilde{v}_k\}_{k=1}^K$ of L_{un} with appropriate normalizations as*

$$\begin{aligned} 0 = \tilde{\mu}_1 &\leq \dots \leq \tilde{\mu}_K, \\ L_{un}\tilde{\mu}_k &= \tilde{\mu}_k\tilde{v}_k, \\ \tilde{v}_k^T\tilde{v}_k &= pN, \quad \tilde{v}_k^T\tilde{v}_l = 0, \quad \forall k \neq l. \end{aligned}$$

Then, as $N \rightarrow \infty$ and $\epsilon \rightarrow 0+$ with $\epsilon \sim \left(\frac{\log N}{N}\right)^{\frac{1}{\frac{d}{2}+2}}$, for sufficiently large N , there exists an event E_1 with probability larger than $1 - cN^{-8}$ such that, on E_1 it holds

$$|\tilde{\mu}_k - \mu_k| \leq C_1 \left(\frac{\log N}{N}\right)^{\frac{1}{\frac{d}{2}+2}}, \quad (2.35)$$

$$\|\tilde{v}_k - \rho_X(\psi_k)\|_\infty \leq C_2 \left(\frac{\log N}{N}\right)^{\frac{1}{d+4}} \quad (2.36)$$

for all $1 \leq k \leq K$, where $\rho_X : C^\infty(\mathcal{M}) \rightarrow \mathbb{R}^N$ is the sampling operator defined as $\rho_X(f) = (f(x_1), \dots, f(x_N))^T$ and c, C_1, C_2 are constants independent of N, ϵ .

Remark 1. *The assumption of single multiplicity for the eigenvalues of the Laplacian Δ in Theorem 1 is introduced primarily for simplicity. This assumption facilitates the derivation of specific eigenvalue and eigenvector approximation errors, as referenced in [16] and further elaborated in the Appendix A. However, it is important to note that such an assumption is not necessary for the theorem's validity. Following the same approach in [16] could bypass*

this assumption. Generally, the eigen-space of Δ may encompass dimensions greater than one, implying that our eigenvector approximation error specified in (2.36) may not directly apply to a predetermined $\{\psi_k\}$ within the eigen-system of Δ . Therefore, the theorem should be understood as asserting the existence of an appropriate orthonormal eigenfunction basis $\{\psi_k\}$ for which the specified eigenvector approximation error (2.36) holds. Such an existence result is sufficient for our purpose.

Drawing from the eigen-consistency results presented in Theorem 1 and leveraging the spectral decomposition (2.9) of the heat kernel, we can craft an estimator for the heat kernel H_t using the following formula:

$$\tilde{H}_{t,K} = \sum_{i=1}^K e^{-\tilde{\mu}_i t} \cdot \tilde{v}_i \tilde{v}_i^T. \quad (2.37)$$

This formulation yields an estimator, $\tilde{H}_{t,K}$, that is essentially an $N \times N$ matrix, approximated across the sample points $\{x_i\}_{i=1}^N$. As highlighted in Theorem 2, each entry of $\tilde{H}_{t,K}$ closely approximates the true heat kernel values at the sampled points, ensuring the estimator's efficacy. The proof of Theorem 2 is reserved for the Appendix B. Similar approaches could be found in [23, 24].

Theorem 2. *Suppose that K, ϵ, N satisfy following conditions:*

$$\left\{ \begin{array}{l} K \geq \left(\frac{d}{C_{low} t} \right)^{\frac{d}{2}} - 1 \\ (K+1)e^{-C_{low}(K+1)^{\frac{2}{d}}t} \leq \frac{1}{K} \\ \epsilon^{\frac{1}{4}} \leq \frac{1}{C_1 C_2 K \mu_K^{\frac{d-1}{2}}} \\ \left(\frac{\log N}{N} \right)^{\frac{1}{\frac{d}{2}+2}} \sim \epsilon \end{array} \right. \quad (2.38)$$

Then, on the event E_1 proposed in Theorem 1, it holds

$$\sup_{i,j \in \{1, \dots, N\}} \left| H_t(x_i, x_j) - \tilde{H}_{t,K}(i, j) \right| \leq \frac{C_a}{K} + C_b \epsilon^{\frac{1}{4}} \quad (2.39)$$

with constants C_a, C_b independent of K, ϵ, N .

Remark 2. *The conditions concerning $K, \epsilon,$ and N , namely the assumption that K is large enough, $\epsilon > 0$ is sufficiently small, and N is adequately large, is to ensure the effectiveness of our heat kernel approximation. It's important to note that, those constants C_1 and C_2 , derived from Theorem 1, are not absolute but depend on K . This implies a sequential approach to parameter selection in a practical algorithm: initially determining K , followed by ϵ , and finally N . However, as [24] have pointed out, the practical application of these theoretical guidelines faces some challenges. The constants tied to the general characteristics of the manifold \mathcal{M} are often difficult to ascertain or control in real-world scenarios. Hence, the practical selection of these hyperparameters— $K, \epsilon,$ and N —typically relies on a trial-and-error approach, rather than a direct application of the theoretical conditions. How to fill the gap between theoretical idealizations and practical feasibility will be a focus of subsequent work.*

3 Main Results

3.1 Diffusion-Based Spectral Algorithm

In this subsection, we introduce our diffusion-based spectral algorithm. Given a labeled dataset $D^l = \{(x_i, y_i)\}_{i=1}^m$ independently and identically distributed from \mathcal{P} on $\mathcal{M} \times \mathbb{R}$ and an unlabeled dataset $D^{ul} = \{x_i\}_{i=m+1}^{m+n}$ i.i.d from ν on \mathcal{M} , we commence by constructing a heat kernel estimator $\tilde{H}_{t,K}$ as in Subsection 2.4 based on the comprehensive input dataset $\{x_i\}_{i=1}^{m+n}$ with $N = m + n$. The estimator $\tilde{H}_{t,K}$ is an $N \times N$ block matrix

$$\tilde{H}_{t,K} = \begin{pmatrix} \tilde{H}_{t,K}^m & \Sigma_{12} \\ \Sigma_{21} & \Sigma_{22} \end{pmatrix}.$$

In this formulation, the first block $\tilde{H}_{t,K}^m$ is an $m \times m$ matrix that effectively approximates the heat kernel for the labeled data points $\{x_i\}_{i=1}^m$, as delineated in Theorem 2. To be more precise, we have

$$\sup_{i,j \in \{1, \dots, m\}} \left| H_t(x_i, x_j) - \tilde{H}_{t,K}^m(i, j) \right| \leq \frac{C_a}{K} + C_b \epsilon^{\frac{1}{4}}.$$

Let $\tilde{H}_{t,m} = \frac{1}{m} \tilde{H}_{t,K}^m$. Leveraging the aforementioned pointwise approximation, an l^∞ -norm error bound between $\tilde{H}_{t,m}$ and the heat kernel matrix H_t as defined previously in (2.29) can be established:

$$\left\| \tilde{H}_{t,m} - H_t \right\|_\infty \leq \frac{1}{m} \left(\frac{C_a}{K} + C_b \epsilon^{\frac{1}{4}} \right). \quad (3.1)$$

This l^∞ -norm error bound paves the way for a consistency result between the eigen-system of $\tilde{H}_{t,m}$ and that of H_t . Notably, since the matrix $\tilde{H}_{t,m}$ is symmetric and positive semi-definite, its eigenvalues can be sorted in a non-increasing order $\tilde{\lambda}_1 \geq \dots \geq \tilde{\lambda}_m \geq 0$. Their corresponding eigenvectors, $\{\tilde{u}_k\}_{k=1}^m$, constitute an orthonormal basis of \mathbb{R}^m . The relationship of those eigens is further explored in Theorem 3, with a proof available in the Appendix C.

Theorem 3. *Suppose that condition (2.38) is satisfied, with E_1 being the event in Theorem 1. Denote*

$$q = \left(\frac{\log m}{C_{up} t (2r + 1)} \right)^{\frac{d}{2}} \quad (3.2)$$

with $r > 1$ a fixed constant. Then, for any $\tau \geq 1$, there exists an event E_2 with probability larger than $1 - 2e^{-\tau}$ such that, on $E_1 \cap E_2$, for any $1 \leq k \leq q$, there hold

$$|\tilde{\lambda}_k - \hat{\lambda}_k| \leq \frac{C_a}{K} + C_b \epsilon^{\frac{1}{4}}, \quad (3.3)$$

$$\|\tilde{u}_k - \hat{u}_k\|_\infty \leq C_c m^{\frac{1}{2r+1}} \left(\frac{1}{K} + \epsilon^{\frac{1}{4}} \right), \quad (3.4)$$

where constants C_a, C_b are the same as in Theorem 2 and C_c is independent of K, ϵ, m , or N .

Theorem 3 suggests that the eigen-pairs of H_t can be effectively replaced by those of $\tilde{H}_{t,m}$ when appropriate hyperparameters are selected. This substitution is reinforced by the

relationship (2.31) between eigens of T_δ and that of H_t , enabling us to define the following data-based empirical eigens

$$\begin{aligned}\tilde{\lambda}_k &= \tilde{\lambda}_k, \\ \tilde{\phi}_k &= \frac{1}{\sqrt{m\tilde{\lambda}_k}} \sum_{i=1}^m \tilde{u}_k(i) \tilde{H}_{t,K}(i, \cdot)\end{aligned}\tag{3.5}$$

as alternatives to the eigenfunctions of the empirical integral operator T_δ . In this definition, $\tilde{H}_{t,K}(i, \cdot)$ denotes the i -th row of the matrix $\tilde{H}_{t,K}$, which is an N -dimensional vector. For clarity, the notation for the eigenvalues of matrix $\tilde{H}_{t,m}$ and the empirical eigenvalue estimators for T_δ remains consistent, reflecting their equivalence. The congruence between $\tilde{\lambda}_k$ and λ_k has been previously established in Theorem 3, since $\lambda_k = \hat{\lambda}_k$ from the relation (2.31). We proceed to demonstrate that the data-based empirical eigenfunction estimator $\tilde{\phi}_k$, represented as an N -dimensional vector, serves as a good approximation of the empirical eigenfunction ϕ_k of T_δ across the full input dataset $\{x_i\}_{i=1}^N$. The accuracy of the approximation is outlined in the upcoming Lemma 2. A proof of this lemma is presented in Appendix D.

Lemma 2. *Suppose that the conditions of Theorem 3 are satisfied, with E_1 being the event in Theorem 1 and E_2 being the event in Theorem 3. Then, on $E_1 \cap E_2$, for any $1 \leq k \leq q$, it holds that*

$$\sup_{1 \leq i \leq N} |\phi_k(x_i) - \tilde{\phi}_k(i)| \leq C_d m^{\frac{r+2}{2r+1}} \left(\frac{1}{K} + \epsilon^{\frac{1}{4}} \right),\tag{3.6}$$

where C_d is a constant independent of K, ϵ, m, N .

Returning to the spectral decomposition representation (2.32) of the spectral algorithm estimator $f_{D,\lambda}$, it is remarkable that

$$\langle g_D, \phi_k \rangle_{\mathcal{H}_t} = \frac{1}{m} \sum_{i=1}^m y_i \langle \phi_k, H_t(x_i, \cdot) \rangle_{\mathcal{H}_t} = \frac{1}{m} \sum_{i=1}^m y_i \phi_k(x_i),$$

which is given by the reproducing property. Consequently, to facilitate our algorithm, we introduce

$$\tilde{g}_{D,k} = \frac{1}{m} \sum_{i=1}^m y_i \tilde{\phi}_k(i)\tag{3.7}$$

as a substitution of $\langle g_D, \phi_k \rangle_{\mathcal{H}_t}$, which is also an N -dimensional vector. With the foundational elements established, we present our diffusion-based spectral algorithm estimator as an approximated-truncated version of the original spectral algorithm:

$$\tilde{f}_{D,\lambda} = \sum_{k=1}^q g_\lambda(\tilde{\lambda}_k) \tilde{g}_{D,k} \tilde{\phi}_k \in \mathbb{R}^N.\tag{3.8}$$

This formulation results in an N -dimensional vector, where the i -th entry provides an estimation of the regression function $f^*(x_i)$ at the i -th data point x_i for all $1 \leq i \leq N$. Emphasizing its capacity as a semi-supervised learning algorithm, our primary interest lies in its performance on the unlabeled input dataset $\{x_i\}_{i=m+1}^{m+n}$, which will be elaborated upon subsequently.

As a comparison, the classical spectral algorithm is typically computed (see e.g. [51, 1]) using the formula

$$f_{D,\lambda} = \frac{1}{m} \sum_{i=1}^m \hat{\gamma}_i H_t(x_i, \cdot),$$

where $\hat{\gamma} = (\hat{\gamma}_1, \dots, \hat{\gamma}_m) \in \mathbb{R}^m$ is determined by

$$\hat{\gamma} = g_\lambda(H_t)y.$$

In this context, H_t represents the heat kernel matrix and $y = (y_1, \dots, y_m) \in \mathbb{R}^m$ denotes the response variables. The computation of $\hat{\gamma}$ necessitates an eigen-decomposition of the entire kernel matrix H_t , which is of dimension m . Our diffusion-based spectral algorithm estimator advances this process by substituting the incalculable heat kernel terms with data-based, calculable estimators and reduces the number of heat kernel matrix eigen-pairs needed from m to q , where q is on the $\log m$ scale. This approach result in a reduction of computational cost while theoretically maintaining learning rates. For insights into similar truncation methods within kernel regression algorithms, references such as [31, 32] are valuable. We conclude this section by presenting our algorithm in Algorithm 1 below.

Algorithm 1 Diffusion-based spectral algorithm

Input: labeled dataset $D^l = \{(x_i, y_i)\}_{i=1}^m$, unlabeled dataset $D^{ul} = \{x_i\}_{i=m+1}^{m+n}$, regularization family $\{g_\lambda\}$, hyperparameters $N = m + n$, ϵ , K , q , λ , t

Output: estimator $\tilde{f}_{D,\lambda}$

Step 1. Compute the un-normalized graph Laplacian L_{un} on $\{x_i\}_{i=1}^N$ by (2.34) with diffusion time ϵ .

Step 2. Compute the eigenvalues $\tilde{\mu}_k$ and eigenvectors \tilde{v}_k of matrix L_{un} with normalization stated in Theorem 1.

Step 3. Compute the heat kernel estimator $\tilde{H}_{t,K}$ by (2.37) with truncation number K .

Step 4. Compute matrix $\tilde{H}_{t,m}$ by selecting first $m \times m$ elements of $\tilde{H}_{t,K}$ with a normalization factor $\frac{1}{m}$.

Step 5. Compute the eigenvalues $\tilde{\lambda}_k$ and eigenvectors \tilde{u}_k of matrix $\tilde{H}_{t,m}$ with normalization stated in Section 3.1.

Step 6. Compute the data-based empirical eigenvalue estimators $\tilde{\lambda}_k$ and eigenfunction estimators $\tilde{\phi}_k$ by (3.5).

Step 7. Compute the diffusion-based spectral algorithm estimator $\tilde{f}_{D,\lambda}$ by (3.7) and (3.8) with regularization family $\{g_\lambda\}$, normalization parameter λ and truncation number q .

3.2 Convergence Results

In this subsection, we delve into the convergence results of our diffusion-based spectral algorithm. This examination begins by introducing several pivotal assumptions essential for establishing a robust analytical foundation.

Assumption 1. *There exists a constant $r > 1$ and a function $g \in \mathcal{H}_t$ such that*

$$f^* = T_\nu^r(g). \tag{3.9}$$

In the convergence analysis of our diffusion-based spectral algorithm, we employ this source condition, a fundamental assumption widely used across various studies in kernel methods and spectral algorithms (see, for instance, [1, 11, 12, 42]). In other words, we adapt the notion of α -power spaces previously introduced in (2.19), to assert that the target regression function $f^* \in \mathcal{H}_t^\beta$ for some $\beta > 3$. This adaptation of the source condition strengthens the classical source

condition, which typically posits $f^* \in \mathcal{H}_t$. The motivation for this enhanced requirement lies in addressing technical considerations within our analysis framework. Nonetheless, it is important to note that this condition could be relaxed back to the classical scenario—or even extended to address harder learning scenarios where $\beta < 1$ —by applying a more intricate approach. The exploration of such scenarios is earmarked for future investigation.

Assumption 2. *There exists a constant $M > 0$ such that, for any sample pair (x, y) distributed from \mathcal{P} on $\mathcal{M} \times \mathbb{R}$, it holds*

$$|y| \leq M. \quad (3.10)$$

This assumption pertains to the boundedness of the conditional distribution of y given x , a premise frequently invoked in statistical learning theory. This boundedness condition, as detailed in [56, 32, 48, 38], provides a foundational constraint that facilitates the development and analysis of learning algorithms by bounding the outcomes within a predictable range. In contrast, some researchers, as seen in [25, 63], opt for a moment condition approach to manage the tail probabilities of the noise term $\epsilon = y - f^*(x)$. This moment condition, which is generally a weaker constraint than the direct boundedness assumption, focuses on controlling the statistical behavior of the noise rather than simply bounding its magnitude. For the purposes of our discussion, the boundedness condition is adopted to simplify the analysis. Although moment condition constraints are weaker, they can still facilitate the derivation of similar results with a little extra effort.

Assumption 3. *The regularization family $\{g_\lambda\}$ has a qualification of $\xi \geq 1$.*

The qualification condition imposed on the regularization family is relatively moderate and can be readily satisfied by various methods. For instance, the examples highlighted in the subsection 2.3 align with this requirement. Additionally, several other notable algorithms, including Landweber iteration, accelerated Landweber iteration, and iterated Tikhonov regularization, also conform to this condition. For further elaboration on these methods and their compliance with the qualification condition, one can refer to [1, 28], where these aspects are discussed in detail.

We now present the convergence analysis for our diffusion-based spectral algorithm in the following Theorem 4.

Theorem 4. *Suppose that Assumption 1, Assumption 2, and Assumption 3 hold. Suppose that condition (2.38) is satisfied with m sufficiently large, $N > K \gg m$ sufficiently large, and $\epsilon \ll 1$ sufficiently small. Denote E_1 the event given in Theorem 1 and E_2 the event given in Theorem 3. Moreover, we choose q as in (3.2) and λ as*

$$\lambda \sim \left(\frac{(\log m)^{\frac{d}{2}}}{m} \right)^{\frac{1}{2}}. \quad (3.11)$$

Then, for any $\tau \geq 1$, there exists an event E_3 with probability larger than $1 - 20e^{-\tau}$ such that, on $E_1 \cap E_2 \cap E_3$, for any $\alpha > 0$ and $m + 1 \leq j \leq m + n$, it holds

$$|\tilde{f}_{D,\lambda}(j) - f^*(x_j)| \leq Cm^{-\theta_1} \cdot (\log m)^{\theta_2} + C'm^{\frac{3}{2r+1}+1} (\log m)^{\frac{d}{2}} \cdot \left(\frac{1}{K} + \epsilon^{\frac{1}{4}} \right), \quad (3.12)$$

where

$$\begin{aligned} \theta_1 &= \min \left\{ \frac{1}{2} \frac{C_{low}}{C_{up}}, \frac{\xi}{2} - \frac{\xi + \frac{1}{2}}{2r + 1} \right\} - \frac{\alpha}{4}, \\ \theta_2 &= \begin{cases} \frac{d\xi}{4} - \frac{d\alpha}{8}, & \text{if } \frac{1}{2} \frac{C_{low}}{C_{up}} \geq \frac{\xi}{2} - \frac{\xi + \frac{1}{2}}{2r + 1} \\ \frac{1}{2} + \frac{d}{4} - \frac{d\alpha}{8}, & \text{if } \frac{1}{2} \frac{C_{low}}{C_{up}} < \frac{\xi}{2} - \frac{\xi + \frac{1}{2}}{2r + 1} \end{cases}, \end{aligned} \quad (3.13)$$

and C, C' are constants independent of $m, K, N, \epsilon, \alpha$.

To elucidate the complex convergence result presented, let us examine two specific cases of the regularization family $\{g_\lambda\}$. For the first example, we select $\{g_\lambda\}$ with a qualification of $\xi = \infty$, a condition met by algorithms such as gradient flow, kernel principal component regularization, and Landweber iteration. In this scenario, according to (3.13), we find that $\theta_1 = \frac{C_{low}}{2C_{up}} - \frac{\alpha}{4}$, where C_{low} and C_{up} are absolute constants related to the eigenvalues of the Laplacian from (2.6). From the proof detailed in section 5, these constants primarily feature in estimating the q -th eigenvalue, μ_q , with $q \rightarrow \infty$ as defined in (3.2), thus they can be considered as functions of q that guide the upper and lower bounds for μ_q . Classical Weyl's law suggests that $\mu_q \sim q^{\frac{2}{d}}$, leading to $\frac{C_{low}}{2C_{up}} \rightarrow \frac{1}{2}$ as $m \rightarrow \infty$. Consequently, the upper bound (3.12) becomes

$$\sup_{1 \leq j \leq N} |\tilde{f}_{D,\lambda}(j) - f^*(x_j)| = \tilde{O} \left(m^{-\frac{1}{2} + \alpha} + m^{\frac{3}{2r+1} + 1} \left(\frac{1}{K} + \left(\frac{\log N}{N} \right)^{\frac{1}{2d+8}} \right) \right), \quad (3.14)$$

with $\alpha > 0$ being arbitrarily small for sufficiently large $m \ll K < N$, focusing only on the main terms. As a second example, consider $g_\lambda(t) = \frac{1}{t+\lambda}$, corresponding to Tikhonov regularization. This choice yields $\xi = 1$, where our upper bounds (3.12) might perform poorly if the regression function f^* lacks sufficient smoothness. However, the Lipschitz continuity of this filter function—a characteristic not common to most filters—allows for a modified proof approach in our Theorem 4, achieving a comparable convergence rate as in (3.14). The detailed proof for Tikhonov regularization's convergence rate is deferred to the Appendix F.

4 Numerical Experiments

In this section, numerical experiments are conducted to showcase the efficacy of the diffusion-based spectral algorithm on a synthetically generated manifold dataset. This dataset is uniformly sampled from the unit sphere S^2 in \mathbb{R}^3 , comprising 1600 data points. These points are divided into a labeled dataset D^l with 140 data points and an unlabeled dataset D^{ul} with 1460 data points. We first consider an intrinsic unit variable regression function, defined as $f^*(\theta) = 20 \sin(\theta) + 24 \cos(\theta)$. For the labeled dataset D^l , the response variable y is generated according to

$$y = f^*(x) + \epsilon,$$

where $\epsilon \sim \mathcal{N}(0, 1)$ denotes Gaussian white noise with unit variance. The experiment evaluates three different filters corresponding to kernel ridge regression, kernel principal component regularization, and gradient flow. Hyperparameters are set by $\epsilon = 10^{-1.4}$, $\lambda = 10^{-4}$, $K =$

200, $q = 80$, and $t = 0.4$ for each filter. The outcomes of these simulations are illustrated in Figure 1. Additionally, a more complex regression function, $f^*(\theta, \phi) = 20 \sin(\theta)\phi$, is examined. This function represents a product of two intrinsic variables, posing a non-trivial regression scenario. Utilizing the same algorithms and parameter settings as before, the results of these simulations are depicted in Figure 2.

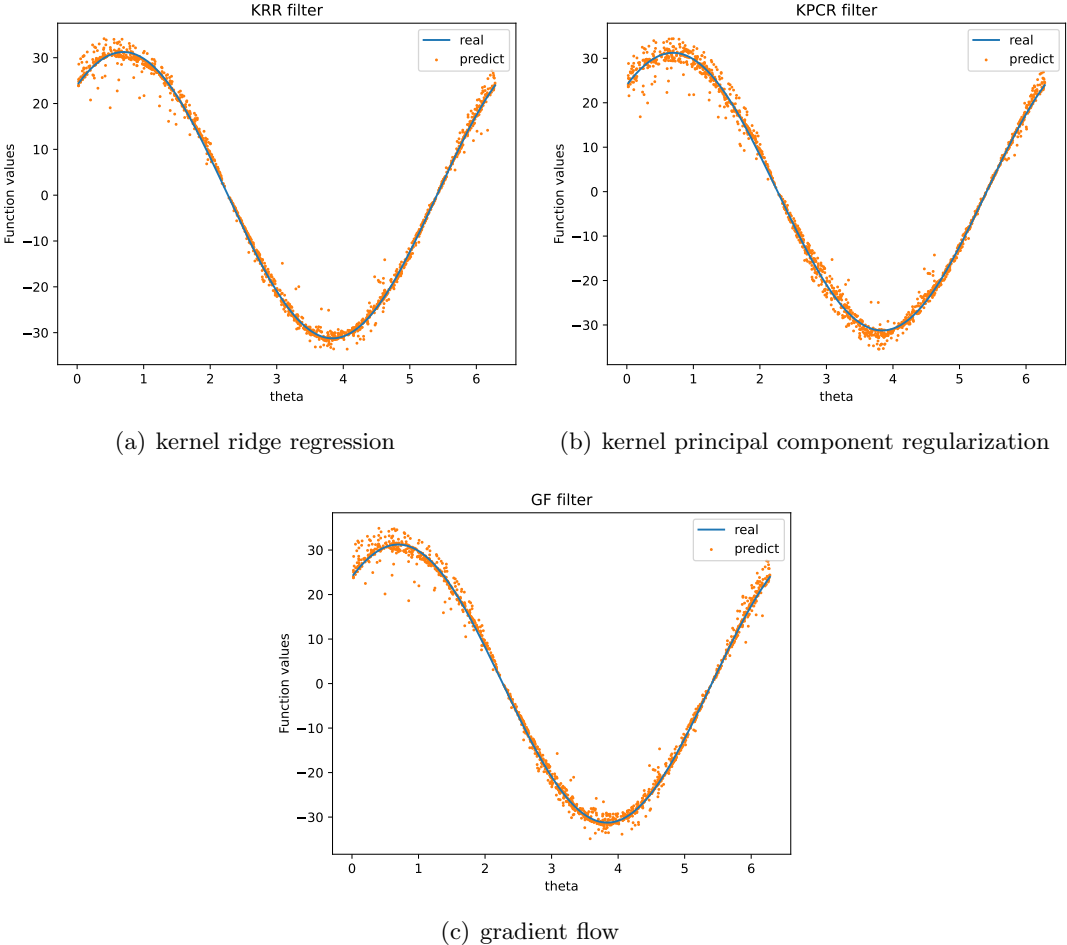


Figure 1: Results for regression function $f^*(\theta) = 20 \sin(\theta) + 24 \cos(\theta)$ on S^2 over a labeled dataset with 140 data points and an unlabeled dataset with 1460 data points. Figure 1(a) illustrates the outcomes of kernel ridge regression, while Figure 1(b) displays the results for kernel principal component regularization, and Figure 1(c) showcases the application of gradient flow. In each depiction, the actual values of f^* are represented by a continuous blue curve, contrasting with the orange scatter points that signify the algorithm’s predictions.

The outcomes of our numerical experiments demonstrate that our diffusion-based spectral algorithm can accurately estimate the regression target function f^* across the entire dataset, comprising both the labeled dataset D^l and the unlabeled dataset D^{ul} , even in scenarios where the labeled dataset is significantly smaller than the unlabeled one, aligning with the predictions made by our theoretical analysis. These findings underscore the algorithm’s efficacy as a semi-supervised learning tool, showing its resilience across various regression functions. Fur-

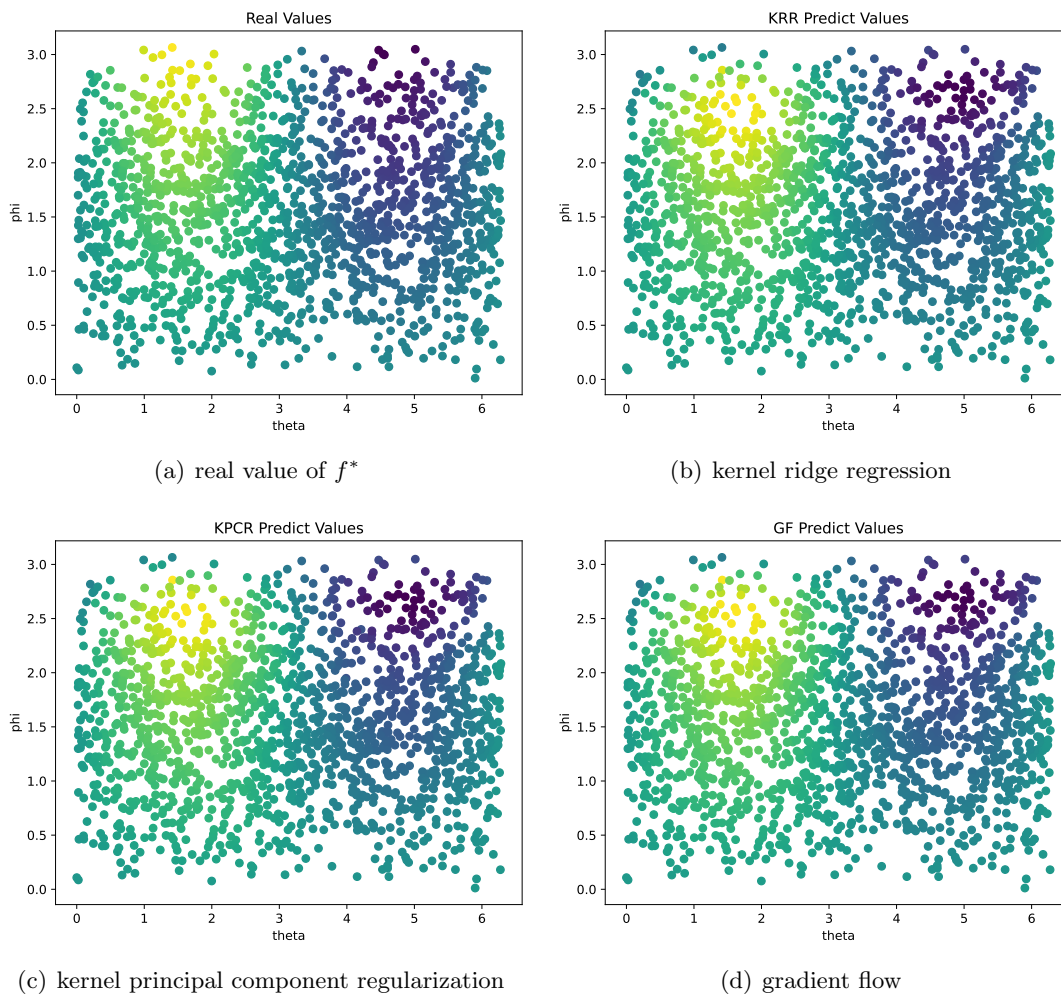


Figure 2: Results for regression function $f^*(\theta, \phi) = 20 \sin(\theta)\phi$ on S^2 over the same dataset with 140 labeled points and 1460 unlabeled points. Figure 2(a) visualizes the true distribution of f^* , serving as a benchmark for comparison. Figures 2(b), 2(c), and 2(d) respectively illustrate the predictions made by kernel ridge regression, kernel principal component regularization, and gradient flow. In these figures, the color assigned to each sample point denotes its response value.

thermore, when comparing the performances of kernel ridge regression (KRR) filters, which possess a qualification of $\xi = 1$, against kernel principal component regularization (KPCR) or gradient flow (GF) filters, which boast a qualification of $\xi = \infty$, we observe negligible differences in their effectiveness. This parity in performance echoes the insights shared in section 3.2, suggesting that our algorithm maintains its robustness across a diverse range of filters. Those results confirm the practical applicability of diffusion-based spectral algorithms in addressing different types of regression challenges in semi-supervised learning contexts.

5 Convergence Analysis

To establish the convergence behaviors for our estimator $\tilde{f}_{D,\lambda}$, which integrates a truncation of the original spectral algorithm estimator $f_{D,\lambda}$ with an approximation of the eigen-system of the empirical integral operator T_δ , we will approach the proof in a segmented manner. First, we will explore the impact of truncating the spectral algorithm estimator in Subsection 5.1, followed by examining the approximation error in Subsection 5.2. Finally, we will synthesize these analyses to establish the desired convergence result in subsection 5.3.

5.1 Truncation Error Analysis

The truncated spectral algorithm estimator $f_{D,\lambda}^T$ is defined as

$$\begin{aligned} f_{D,\lambda}^T &= \sum_{k=1}^q g_\lambda(\lambda_k) \langle g_D, \phi_k \rangle_{\mathcal{H}_t} \cdot \phi_k \\ &= g_\lambda(T_\delta) g_D^T, \end{aligned} \quad (5.1)$$

where

$$g_D^T = \sum_{k=1}^q \langle g_D, \phi_k \rangle_{\mathcal{H}_t} \phi_k \quad (5.2)$$

represents the truncation of g_D . Given any $\alpha > 0$, we focus on the α -power norm error $\|f_{D,\lambda}^T - f^*\|_\alpha$. Recall that

$$f_{D,\lambda} = g_\lambda(T_\delta) g_D.$$

We introduce

$$\hat{f}_{D,\lambda} = g_\lambda(T_\delta) T_\delta f^*. \quad (5.3)$$

This allows us to break down the original truncation error into three distinct components:

$$\begin{aligned} \|f_{D,\lambda}^T - f^*\|_\alpha &\leq \|f_{D,\lambda}^T - \hat{f}_{D,\lambda}\|_\alpha + \|\hat{f}_{D,\lambda} - f_{D,\lambda}\|_\alpha + \|f_{D,\lambda} - f^*\|_\alpha \\ &\triangleq I_1 + I_2 + I_3. \end{aligned}$$

Next, we will address these three terms individually.

Lemma 3. *Suppose that $0 < \alpha \leq 1$, $\tau \geq 1$. We choose q, λ as in (3.2) and (3.11) separately and m sufficiently large. Then, with probability larger than $1 - 10e^{-\tau}$, it holds*

$$I_1 \leq K_1 m^{-\frac{C_{low}}{C_{up}} \cdot \frac{1}{2} + \frac{\alpha}{4}} (\log m)^{\frac{1}{2} + \frac{d}{4} - \frac{\alpha d}{8}}$$

with K_1 a constant independent of m, α .

Proof. Drawing from [25], we have that for any $0 < \alpha \leq 1$ and for any function $f \in \mathcal{H}_t$,

$$\|f\|_\alpha = \|T_\nu^{\frac{1-\alpha}{2}} f\|_{\mathcal{H}_t}.$$

This leads to

$$\begin{aligned} \|f_{D,\lambda}^T - \hat{f}_{D,\lambda}\|_\alpha &= \|T_\nu^{\frac{1-\alpha}{2}} (f_{D,\lambda}^T - \hat{f}_{D,\lambda})\|_{\mathcal{H}_t} \\ &\leq \|T_\nu^{\frac{1-\alpha}{2}} (T_\nu + \lambda I)^{-\frac{1}{2}}\|_{\mathcal{B}(\mathcal{H}_t)} \cdot \|(T_\nu + \lambda I)^{\frac{1}{2}} (f_{D,\lambda}^T - \hat{f}_{D,\lambda})\|_{\mathcal{H}_t}. \end{aligned}$$

We provide an explanation for the symbols adopted here. Let $(\mathcal{H}, \langle \cdot, \cdot \rangle_{\mathcal{H}})$ and $(\mathcal{H}', \langle \cdot, \cdot \rangle_{\mathcal{H}'})$ be two Hilbert spaces. Therefore, the collection of bounded linear operators from \mathcal{H} to \mathcal{H}' forms a Banach space, symbolized as $\mathcal{B}(\mathcal{H}, \mathcal{H}')$ with operator norm $\|A\|_{\mathcal{B}(\mathcal{H}, \mathcal{H}')} = \sup_{\|f\|_{\mathcal{H}}=1} \|Af\|_{\mathcal{H}'}$. In the special case $\mathcal{H} = \mathcal{H}'$, we denote it as $\mathcal{B}(\mathcal{H})$ with the corresponding operator norm given by $\|A\|_{\mathcal{B}(\mathcal{H})}$. Furthermore,

$$\|T_\nu^{\frac{1-\alpha}{2}} (T_\nu + \lambda I)^{-\frac{1}{2}}\|_{\mathcal{B}(\mathcal{H}_t)} = \sup_{k \geq 1} \left(\frac{p^{1-\alpha} e^{-t\mu_k(1-\alpha)}}{pe^{-t\mu_k} + \lambda} \right)^{\frac{1}{2}} \leq \lambda^{-\frac{\alpha}{2}}. \quad (5.4)$$

The last inequality in this sequence is derived from a straightforward calculation involving the function $t \mapsto t^{1-\alpha}/(\lambda + t)$. For the remaining term, we further decompose it as

$$\begin{aligned} \|(T_\nu + \lambda I)^{\frac{1}{2}} (f_{D,\lambda}^T - \hat{f}_{D,\lambda})\|_{\mathcal{H}_t} &= \|(T_\nu + \lambda I)^{\frac{1}{2}} g_\lambda(T_\delta) (g_D^T - T_\delta f^*)\|_{\mathcal{H}_t} \\ &\leq \|(T_\nu + \lambda I)^{\frac{1}{2}} (T_\delta + \lambda I)^{-\frac{1}{2}}\|_{\mathcal{B}(\mathcal{H}_t)} \\ &\quad \cdot \|(T_\delta + \lambda I)^{\frac{1}{2}} g_\lambda(T_\delta) (T_\delta + \lambda I)^{\frac{1}{2}}\|_{\mathcal{B}(\mathcal{H}_t)} \\ &\quad \cdot \|(T_\delta + \lambda I)^{-\frac{1}{2}} (g_D^T - T_\delta f^*)\|_{\mathcal{H}_t}. \end{aligned} \quad (5.5)$$

Also drawing from [25], it is established that, with probability larger than $1 - 2e^{-\tau}$, for sufficiently large m ,

$$\|(T_\nu + \lambda I)^{\frac{1}{2}} (T_\delta + \lambda I)^{-\frac{1}{2}}\|_{\mathcal{B}(\mathcal{H}_t)} \leq \sqrt{3}. \quad (5.6)$$

Additionally, by leveraging the characteristics of the filter function g_λ , as described in (2.25), we have

$$\|(T_\delta + \lambda I)^{\frac{1}{2}} g_\lambda(T_\delta) (T_\delta + \lambda I)^{\frac{1}{2}}\|_{\mathcal{B}(\mathcal{H}_t)} = \|(T_\delta + \lambda I) g_\lambda(T_\delta)\|_{\mathcal{B}(\mathcal{H}_t)} \leq 2. \quad (5.7)$$

As for the last term (5.5), we exploit the following decomposition

$$\begin{aligned} \|(T_\delta + \lambda I)^{-\frac{1}{2}} (g_D^T - T_\delta f^*)\|_{\mathcal{H}_t} &= \left\| \sum_{k=1}^q (\lambda_k + \lambda)^{-\frac{1}{2}} (\langle g_D, \phi_k \rangle_{\mathcal{H}_t} - \langle T_\delta f^*, \phi_k \rangle_{\mathcal{H}_t}) \phi_k \right\|_{\mathcal{H}_t} \\ &\quad + \left\| \sum_{k=q+1}^{\infty} (\lambda_k + \lambda)^{-\frac{1}{2}} \langle T_\delta f^*, \phi_k \rangle_{\mathcal{H}_t} \phi_k \right\|_{\mathcal{H}_t} \\ &= \left(\sum_{k=1}^q (\lambda_k + \lambda)^{-1} (\langle g_D, \phi_k \rangle_{\mathcal{H}_t} - \langle T_\delta f^*, \phi_k \rangle_{\mathcal{H}_t})^2 \right)^{\frac{1}{2}} \\ &\quad + \left(\sum_{k=q+1}^{\infty} (\lambda_k + \lambda)^{-1} \lambda_k^2 \langle f^*, \phi_k \rangle_{\mathcal{H}_t}^2 \right)^{\frac{1}{2}} \\ &\triangleq J_1 + J_2, \end{aligned}$$

where the second equation follows from $T_\delta f^* = \sum \lambda_l \langle f^*, \phi_l \rangle \phi_l$. We consider J_1 first. Notice that

$$\begin{aligned} |\langle g_D, \phi_k \rangle_{\mathcal{H}_t} - \langle T_\delta f^*, \phi_k \rangle_{\mathcal{H}_t}| &= |\langle g_D, \phi_k \rangle_{\mathcal{H}_t} - \lambda_k \langle f^*, \phi_k \rangle_{\mathcal{H}_t}| \\ &= \sqrt{\lambda_k} \sqrt{\lambda_k} \left| \left\langle \frac{1}{\lambda_k} g_D, \phi_k \right\rangle_{\mathcal{H}_t} - \langle f^*, \phi_k \rangle_{\mathcal{H}_t} \right|. \end{aligned}$$

From [32] we have, with probability larger than $1 - 2e^{-\tau}$, for any $k \in \mathbb{N}$,

$$\sqrt{\lambda_k} \left| \left\langle \frac{1}{\lambda_k} g_D, \phi_k \right\rangle_{\mathcal{H}_t} - \langle f^*, \phi_k \rangle_{\mathcal{H}_t} \right| \leq 3M \sqrt{\frac{\log m}{m}}.$$

Therefore, a combination with (3.2) yields

$$\begin{aligned} J_1 &\leq \left(\sum_{k=1}^q (\lambda_k + \lambda)^{-1} \lambda_k \cdot 9M^2 \frac{\log m}{m} \right)^{\frac{1}{2}} \\ &\leq \sqrt{q} \cdot 3M \sqrt{\frac{\log m}{m}} \\ &\lesssim m^{-\frac{1}{2}} (\log m)^{\frac{1}{2} + \frac{d}{4}}. \end{aligned} \tag{5.8}$$

Here, $A \lesssim B$ implies that A is less than or equal to B up to a multiplication of constant. We now turn to J_2 . According to [32] again, we have, with probability larger than $1 - 6e^{-\tau}$,

$$J_2 \leq C_J \left\{ \min \left\{ \frac{\Lambda_{m,q}}{\sqrt{\lambda}}, \Lambda_{m,q}^{\frac{1}{2}} \right\} \gamma_q^r + \frac{\gamma_q}{(2\lambda + \gamma_q)^{\frac{1}{2}}} \frac{1}{\sqrt{m}} + 2^r \Lambda_{m,q}^{\frac{1}{2}} \left[\left(\sum_{k=q+1}^{\infty} \gamma_k^{2r} \right)^{\frac{1}{2}} + \frac{8}{\sqrt{m}} \right] \right\}.$$

Here, $\Lambda_{m,q} = \max \left\{ \frac{\gamma_q}{\kappa^2}, \frac{1}{\sqrt{m}} \right\}$, $\gamma_k = pe^{-t\mu_k}$ is an abbreviation, and C_J is a constant independent of m . In the following discussions, we will estimate above three terms separately. Recall that

$$q = \left(\frac{\log m}{C_{up} t (2r+1)} \right)^{\frac{d}{2}}, \quad \lambda \sim \left(\frac{(\log m)^{\frac{d}{2}}}{m} \right)^{\frac{1}{2}}.$$

Hence we have

$$\Lambda_{m,q} \leq \max \left\{ \frac{1}{\sqrt{m}}, \frac{p}{\kappa^2} \left(\frac{1}{m} \right)^{\frac{C_{low}}{C_{up}} \frac{1}{2r+1}} \right\} \lesssim m^{-\frac{C_{low}}{C_{up}} \frac{1}{2r+1}},$$

and

$$\frac{\Lambda_{m,q}}{\sqrt{\lambda}} \lesssim (\log m)^{-\frac{d}{8}} \cdot m^{-\frac{C_{low}}{C_{up}} \frac{1}{2r+1} + \frac{1}{4}}.$$

Since $\frac{C_{low}}{C_{up}} \frac{1}{2r+1} < \frac{1}{2}$, we derive that

$$\min \left\{ \frac{\Lambda_{m,q}}{\sqrt{\lambda}}, \Lambda_{m,q}^{\frac{1}{2}} \right\} \lesssim m^{-\frac{C_{low}}{C_{up}} \frac{1}{2r+1} \cdot \frac{1}{2}}.$$

Therefore,

$$\min \left\{ \frac{\Lambda_{m,q}}{\sqrt{\lambda}}, \Lambda_{m,q}^{\frac{1}{2}} \right\} \gamma_q^r \lesssim m^{-\frac{C_{low}}{C_{up}} \frac{1}{2r+1} \cdot \frac{1}{2}} \cdot m^{-\frac{C_{low}}{C_{up}} \frac{r}{2r+1}} \lesssim m^{-\frac{C_{low}}{C_{up}} \cdot \frac{1}{2}}. \tag{5.9}$$

Further, from $r > 1$ we have

$$2\lambda + \gamma_q \gtrsim \gamma_q.$$

Hence

$$\frac{\gamma_q}{(2\lambda + \gamma_q)^{\frac{1}{2}}} \frac{1}{\sqrt{m}} \lesssim \gamma_q^{\frac{1}{2}} \frac{1}{\sqrt{m}} \lesssim m^{-\frac{C_{low}}{C_{up}} \frac{1}{2r+1} \cdot \frac{1}{2} - \frac{1}{2}}. \quad (5.10)$$

For the last term, similar to the calculation (C.5) for $\Lambda_{>l}$ in the Appendix C, we have

$$\sum_{k=q+1}^{\infty} \gamma_k^{2r} = \sum_{k=q+1}^{\infty} (pe^{-\mu_k t})^{2r} \lesssim q(pe^{-\mu_q t})^{2r} \lesssim m^{-\frac{C_{low}}{C_{up}} \frac{2r}{2r+1}} (\log m)^{\frac{d}{2}},$$

which results in

$$\left(\sum_{k=q+1}^{\infty} \gamma_k^{2r} \right)^{\frac{1}{2}} + \frac{8}{\sqrt{m}} \lesssim m^{-\frac{C_{low}}{C_{up}} \frac{r}{2r+1}} (\log m)^{\frac{d}{4}} + m^{-\frac{1}{2}} \lesssim m^{-\frac{C_{low}}{C_{up}} \frac{r}{2r+1}} (\log m)^{\frac{d}{4}}.$$

Therefore,

$$\begin{aligned} 2^r \Lambda_{m,q}^{\frac{1}{2}} \left[\left(\sum_{k=q+1}^{\infty} \gamma_k^{2r} \right)^{\frac{1}{2}} + \frac{8}{\sqrt{m}} \right] &\lesssim m^{-\frac{C_{low}}{C_{up}} \frac{\frac{1}{2}}{2r+1}} \cdot m^{-\frac{C_{low}}{C_{up}} \frac{r}{2r+1}} (\log m)^{\frac{d}{4}} \\ &\lesssim m^{-\frac{C_{low}}{C_{up}} \cdot \frac{1}{2}} (\log m)^{\frac{d}{4}}. \end{aligned} \quad (5.11)$$

Therefore, a combination of (5.9), (5.10), and (5.11) yields

$$J_2 \lesssim m^{-\frac{C_{low}}{C_{up}} \cdot \frac{1}{2}} (\log m)^{\frac{d}{4}}. \quad (5.12)$$

Finally, combining (5.8), (5.12) with (5.4), (5.6), and (5.7) we derive

$$\begin{aligned} \|f_{D,\lambda}^T - \hat{f}_{D,\lambda}\|_{\alpha} &\lesssim \left(\frac{(\log m)^{\frac{d}{2}}}{m} \right)^{\frac{1}{2} \cdot \frac{1}{2} - \frac{\alpha}{2}} \cdot \left(m^{-\frac{1}{2}} (\log m)^{\frac{1}{2} + \frac{d}{4}} + m^{-\frac{C_{low}}{C_{up}} \cdot \frac{1}{2}} (\log m)^{\frac{d}{4}} \right) \\ &\lesssim m^{-\frac{C_{low}}{C_{up}} \cdot \frac{1}{2} + \frac{\alpha}{4}} (\log m)^{\frac{1}{2} + \frac{d}{4} - \frac{\alpha d}{8}}, \end{aligned}$$

which completes the proof. \square

Lemma 4. *Suppose that $0 < \alpha \leq 1$, $\tau \geq 1$, λ chosen as in (3.11), and m sufficiently large. Then, with probability at least $1 - 6e^{-\tau}$, it holds*

$$I_2 \leq K_2 m^{-\frac{1}{2} + \frac{\alpha}{4}} (\log m)^{\frac{d}{4} - \frac{\alpha d}{8}},$$

where K_2 is a constant independent of m or α .

Proof. From (2.27) and (5.3) we have

$$f_{D,\lambda} - \hat{f}_{D,\lambda} = g_{\lambda}(T_{\delta})(g_D - T_{\delta} f^*).$$

Therefore,

$$\begin{aligned} \|f_{D,\lambda} - \hat{f}_{D,\lambda}\|_\alpha &= \|T_\nu^{\frac{1-\alpha}{2}}(f_{D,\lambda} - \hat{f}_{D,\lambda})\|_{\mathcal{H}_t} \\ &\leq \|T_\nu^{\frac{1-\alpha}{2}}(T_\nu + \lambda I)^{-\frac{1}{2}}\|_{\mathcal{B}(\mathcal{H}_t)} \cdot \|(T_\nu + \lambda I)^{\frac{1}{2}}(T_\delta + \lambda I)^{-\frac{1}{2}}\|_{\mathcal{B}(\mathcal{H}_t)} \\ &\quad \cdot \|(T_\delta + \lambda I)^{\frac{1}{2}}(f_{D,\lambda} - \hat{f}_{D,\lambda})\|_{\mathcal{H}_t}. \end{aligned}$$

It is remarkable that the first two terms have already been bounded in (5.4) and (5.6). For the remaining term, we further decompose it as

$$\begin{aligned} \|(T_\delta + \lambda I)^{\frac{1}{2}}(f_{D,\lambda} - \hat{f}_{D,\lambda})\|_{\mathcal{H}_t} &= \|(T_\delta + \lambda I)^{\frac{1}{2}}g_\lambda(T_\delta)(g_D - T_\delta f^*)\|_{\mathcal{H}_t} \\ &\leq \|(T_\delta + \lambda I)^{\frac{1}{2}}g_\lambda(T_\delta)(T_\delta + \lambda I)^{\frac{1}{2}}\|_{\mathcal{B}(\mathcal{H}_t)} \\ &\quad \cdot \|(T_\delta + \lambda I)^{-\frac{1}{2}}(T_\nu + \lambda I)^{\frac{1}{2}}\|_{\mathcal{B}(\mathcal{H}_t)} \\ &\quad \cdot \|(T_\nu + \lambda I)^{-\frac{1}{2}}(g_D - T_\delta f^*)\|_{\mathcal{H}_t} \end{aligned}$$

with the first two terms also discussed in (5.7) and (5.6). To facilitate the third term above, we introduce a continuous version of $f_{D,\lambda}$ as

$$f_{P,\lambda} = g_\lambda(T_\nu)g_P. \quad (5.13)$$

Here,

$$g_P \triangleq I_\nu^* f^* = \int_{\mathcal{M} \times \mathbb{R}} y H_t(x, \cdot) d\mathcal{P}(x, y).$$

As a result, we further control it by

$$\begin{aligned} \|(T_\nu + \lambda I)^{-\frac{1}{2}}(g_D - T_\delta f^*)\|_{\mathcal{H}_t} &\leq \|(T_\nu + \lambda I)^{-\frac{1}{2}}(g_D - T_\delta f_{P,\lambda})\|_{\mathcal{H}_t} \\ &\quad + \|(T_\nu + \lambda I)^{-\frac{1}{2}}T_\delta(f_{P,\lambda} - f^*)\|_{\mathcal{H}_t}. \end{aligned}$$

Drawing from Lemma 10 of [62] with $\beta = 2$, it is shown that with probability larger than $1 - 2e^{-\tau}$,

$$\left\| (T_\nu + \lambda I)^{-\frac{1}{2}}(g_D - T_\delta f_{P,\lambda}) \right\|_{\mathcal{H}_t}^2 \lesssim \frac{1}{m} \left(N_\nu(\lambda) + \lambda^{2-\alpha} + \frac{L_\lambda^2}{m\lambda^\alpha} \right) + \lambda^2. \quad (5.14)$$

Here, $N_\nu(\lambda) = \text{tr}((T_\nu + \lambda I)^{-1}T_\nu)$ and $L_\lambda = \max\{M, \|f_{P,\lambda} - f^*\|_\infty\}$. Notably, while the original Lemma 10 in [62] is formulated for $\beta \leq 1$, it can be adapted for $\beta = 2$, an extension that will be detailed in the Appendix E. Employing methodologies akin to those in the proof of Theorem 1 in [62], with $\lambda \sim \left(\frac{(\log m)^{\frac{d}{2}}}{m}\right)^{\frac{1}{2}}$ corresponding to $\beta = 2$ (Again note that the original theorem addressed $\beta \leq 1$, which yet can be extended to $\beta = 2$. We will formulate this in Appendix E), which now results in

$$\left\| (T_\nu + \lambda I)^{-\frac{1}{2}}(g_D - T_\delta f_{P,\lambda}) \right\|_{\mathcal{H}_t} \lesssim \lambda. \quad (5.15)$$

We decompose the remaining term as

$$\begin{aligned} \|(T_\nu + \lambda I)^{-\frac{1}{2}}T_\delta(f_{P,\lambda} - f^*)\|_{\mathcal{H}_t} &\leq \|(T_\nu + \lambda I)^{-\frac{1}{2}}(T_\delta - T_\nu)(f_{P,\lambda} - f^*)\|_{\mathcal{H}_t} \\ &\quad + \|(T_\nu + \lambda I)^{-\frac{1}{2}}T_\nu(f_{P,\lambda} - f^*)\|_{\mathcal{H}_t} \\ &\triangleq J_1 + J_2. \end{aligned}$$

For J_1 , we have

$$J_1 \leq \|(T_\nu + \lambda I)^{-\frac{1}{2}}\|_{\mathcal{B}(\mathcal{H}_t)} \cdot \|T_\delta - T_\nu\|_{\mathcal{B}(\mathcal{H}_t)} \cdot \|f_{P,\lambda} - f^*\|_{\mathcal{H}_t}.$$

A direct computation yields

$$\|(T_\nu + \lambda I)^{-\frac{1}{2}}\|_{\mathcal{B}(\mathcal{H}_t)} = \sup_{k \geq 1} \left(\frac{1}{pe^{-t\mu_k} + \lambda} \right)^{\frac{1}{2}} \leq \lambda^{-\frac{1}{2}}.$$

Drawing from [32] we have, with probability larger than $1 - 2e^{-\tau}$,

$$\|T_\delta - T_\nu\|_{\mathcal{B}(\mathcal{H}_t)} \leq \|T_\delta - T_\nu\|_{HS} \leq C_h \tau m^{-\frac{1}{2}}.$$

with $\|\cdot\|_{HS}$ the Hilbert-Schmidt norm and C_h a constant independent of m, τ . Moreover, [25] proves that

$$\|f_{P,\lambda} - f^*\|_{\mathcal{H}_t} \leq \|f^*\|_2 \lambda^{\frac{1}{2}}.$$

Combining the above yields

$$J_1 \lesssim m^{-\frac{1}{2}}. \quad (5.16)$$

As for J_2 , we have

$$\begin{aligned} J_2 &= \|(T_\nu + \lambda I)^{-\frac{1}{2}} T_\nu (f_{P,\lambda} - f^*)\|_{\mathcal{H}_t} \\ &= \|(T_\nu + \lambda I)^{-\frac{1}{2}} I_\nu^* I_\nu (f_{P,\lambda} - f^*)\|_{\mathcal{H}_t} \\ &\leq \|(T_\nu + \lambda I)^{-\frac{1}{2}} I_\nu^*\|_{\mathcal{B}(L^2(\nu), \mathcal{H}_t)} \cdot \|f_{P,\lambda} - f^*\|_{L^2(\nu)}. \end{aligned}$$

Notic that

$$\|(T_\nu + \lambda I)^{-\frac{1}{2}} I_\nu^*\|_{\mathcal{B}(L^2(\nu), \mathcal{H}_t)} = \sup_{k \geq 0} \left(\frac{pe^{-t\mu_k}}{pe^{-t\mu_k} + \lambda} \right)^{\frac{1}{2}} \leq 1,$$

and [25] shows that

$$\|f_{P,\lambda} - f^*\|_{L^2(\nu)} \leq \|f^*\|_2 \lambda.$$

Therefore,

$$J_2 \lesssim \lambda. \quad (5.17)$$

Finally, combining (5.15), (5.16), and (5.17) with former results (5.4), (5.6), and (5.7), we derive that

$$\|f_{D,\lambda} - \hat{f}_{D,\lambda}\|_\alpha \lesssim \lambda^{-\frac{\alpha}{2}} \cdot \left(m^{-\frac{1}{2}} + \lambda \right) \lesssim \lambda^{1-\frac{\alpha}{2}} \lesssim m^{-\frac{1}{2} + \frac{\alpha}{4}} (\log m)^{\frac{d}{4} - \frac{\alpha d}{8}},$$

which completes the proof. \square

Utilizing Theorem 1 in [62] with $\beta = 2$ and $\gamma = \alpha$ (Similarly, we have to extend the original result from $\beta \leq 1$ to $\beta = 2$, same as in the derivation of (5.15)), we have

Lemma 5. *Suppose that $0 < \alpha \leq 1$, $\tau \geq 1$, λ chosen as in (3.11), m sufficiently large. Then, with probability at least $1 - 4e^{-\tau}$, it holds*

$$I_3 \leq K_3 m^{-\frac{1}{2} + \frac{\alpha}{4}} (\log m)^{\frac{d}{4} - \frac{\alpha d}{8}},$$

where K_3 is a constant independent of m, α .

Finally, a combination of above Lemma 3, Lemma 4, and Lemma 5 yields the following result:

$$\begin{aligned} \|f_{D,\lambda}^T - f^*\|_\alpha &\lesssim m^{-\frac{C_{low}}{C_{up}} \cdot \frac{1}{2} + \frac{\alpha}{4}} (\log m)^{\frac{1}{2} + \frac{d}{4} - \frac{\alpha d}{8}} + m^{-\frac{1}{2} + \frac{\alpha}{4}} (\log m)^{\frac{d}{4} - \frac{\alpha d}{8}} \\ &\lesssim m^{-\frac{C_{low}}{C_{up}} \cdot \frac{1}{2} + \frac{\alpha}{4}} (\log m)^{\frac{1}{2} + \frac{d}{4} - \frac{\alpha d}{8}}, \end{aligned}$$

which is valid for all $0 < \alpha \leq 1$. Drawing from [62], $\mathcal{H}_t^\alpha \hookrightarrow L^\infty(\nu)$ holds for all $\alpha > 0$. Therefore, the following Theorem 5 is a direct corollary of above results.

Theorem 5. *Suppose that Assumption 1, Assumption 2, and Assumption 3 hold. We choose q, λ as in (3.2) and (3.11) separately. Then, for any $0 < \alpha \leq 1$ and $\tau \geq 1$, when m large enough, there exists an event E_3 with probability larger than $1 - 20e^{-\tau}$ such that, on E_3 it holds*

$$\|f_{D,\lambda}^T - f^*\|_\infty \leq K_t m^{-\frac{C_{low}}{C_{up}} \cdot \frac{1}{2} + \frac{\alpha}{4}} (\log m)^{\frac{1}{2} + \frac{d}{4} - \frac{\alpha d}{8}}.$$

Here, K_t is a constant independent of m, α .

5.2 Approximation Error Analysis

In this subsection, we establish the point-wise upper bound between the truncated spectral algorithm estimator $f_{D,\lambda}^T$, as defined in (5.1), and our diffusion-based spectral algorithm estimator $\tilde{f}_{D,\lambda}$. For any $1 \leq j \leq N$, we begin by decomposing the error into distinct components:

$$\begin{aligned} |f_{D,\lambda}^T(x_j) - \tilde{f}_{D,\lambda}(j)| &= \left| \sum_{k=1}^q g_\lambda(\lambda_k) \langle g_D, \phi_k \rangle_{\mathcal{H}_t} \phi_k(x_j) - \sum_{k=1}^q g_\lambda(\tilde{\lambda}_k) \tilde{g}_{D,k} \tilde{\phi}_k(j) \right| \\ &\leq \left| \sum_{k=1}^q \left(g_\lambda(\lambda_k) - g_\lambda(\tilde{\lambda}_k) \right) \langle g_D, \phi_k \rangle_{\mathcal{H}_t} \phi_k(x_j) \right| \\ &\quad + \left| \sum_{k=1}^q g_\lambda(\tilde{\lambda}_k) \left(\langle g_D, \phi_k \rangle_{\mathcal{H}_t} \phi_k(x_j) - \tilde{g}_{D,k} \tilde{\phi}_k(j) \right) \right| \\ &\triangleq I_1 + I_2. \end{aligned}$$

We will first address the upper bound for I_1 , our approach and findings are presented in the following Lemma 6.

Lemma 6. *Suppose that Assumption 1, Assumption 2, and Assumption 3 hold. Suppose that the conditions (2.38) holds with m sufficiently large, $N > K \gg m$ sufficiently large and ϵ sufficiently small. We choose q, λ as in (3.2) and (3.11) separately. Denote E_1 the event given in Theorem 1, E_2 the event given in Theorem 3 and E_3 the event given in Theorem 5. Then, on $E_1 \cap E_2 \cap E_3$, for any $0 < \alpha \leq 1$ and $1 \leq j \leq N$, it holds*

$$I_1 \leq K'_1 \left(m^{-\frac{\xi}{2} + \frac{1}{2r+1}(\xi + \frac{1}{2}) + \frac{\alpha}{4}} \cdot (\log m)^{\frac{d\xi}{4} - \frac{d\alpha}{8}} + m^{\frac{1}{2r+1} \cdot \frac{3}{2} + \frac{\alpha}{4}} \cdot (\log m)^{-\frac{d\alpha}{8}} \cdot \left(\frac{1}{K} + \epsilon^{\frac{1}{4}} \right) \right),$$

where K'_1 is a constant independent of $m, K, N, \epsilon, \alpha$.

Proof. Recalling the empirical eigen-system as defined in (2.28), we obtain the spectral decomposition for T_δ :

$$T_\delta = \sum_{k=1}^{\infty} \lambda_k \langle \cdot, \phi_k \rangle_{\mathcal{H}_t} \phi_k.$$

Subsequently, we introduce

$$\tilde{T}_\delta = \sum_{k=1}^{\infty} \tilde{\lambda}_k \langle \cdot, \phi_k \rangle_{\mathcal{H}_t} \phi_k,$$

where $\tilde{\lambda}_k = 0$ for $k > m$. Then we have

$$I_1 = \left| g_\lambda(T_\delta) g_D^T(x_j) - g_\lambda(\tilde{T}_\delta) g_D^T(x_j) \right| \leq \left\| \left(g_\lambda(T_\delta) - g_\lambda(\tilde{T}_\delta) \right) g_D^T \right\|_\infty.$$

Adopting a strategy parallel to the one adopted in Subsection 5.1, we commence our analysis by examining the $\|\cdot\|_\alpha$ -norm bound, subsequently deriving the $\|\cdot\|_\infty$ -norm bound through embedding results. Initially, we break down the error into

$$\begin{aligned} \left\| \left(g_\lambda(T_\delta) - g_\lambda(\tilde{T}_\delta) \right) g_D^T \right\|_\alpha &= \left\| T_\nu^{\frac{1-\alpha}{2}} \left(g_\lambda(T_\delta) - g_\lambda(\tilde{T}_\delta) \right) g_D^T \right\|_{\mathcal{H}_t} \\ &\leq \|T_\nu^{\frac{1-\alpha}{2}} (T_\nu + \lambda I)^{-\frac{1}{2}}\|_{\mathcal{B}(\mathcal{H}_t)} \\ &\quad \cdot \left\| (T_\nu + \lambda I)^{\frac{1}{2}} \left(g_\lambda(T_\delta) - g_\lambda(\tilde{T}_\delta) \right) g_D^T \right\|_{\mathcal{H}_t}, \end{aligned}$$

where the first term is bounded by $\lambda^{-\frac{\alpha}{2}}$ as in (5.4). Now, let's introduce several abbreviations:

$$\begin{aligned} f_1 &= g_\lambda(T_\delta) g_D^T, \\ f_2 &= g_\lambda(\tilde{T}_\delta) g_D^T, \\ h_\lambda(t) &= 1 - t g_\lambda(t). \end{aligned}$$

Therefore,

$$\begin{aligned} f_1 - f_2 &= f_1 - (h_\lambda(T_\delta) + T_\delta g_\lambda(T_\delta)) f_2 \\ &= g_\lambda(T_\delta) (g_D^T - T_\delta f_2) - h_\lambda(T_\delta) f_2. \end{aligned}$$

As a consequence, we further decompose the remaining term as

$$\begin{aligned} \left\| (T_\nu + \lambda I)^{\frac{1}{2}} \left(g_\lambda(T_\delta) - g_\lambda(\tilde{T}_\delta) \right) g_D^T \right\|_{\mathcal{H}_t} &\leq \left\| (T_\nu + \lambda I)^{\frac{1}{2}} g_\lambda(T_\delta) (g_D^T - T_\delta f_2) \right\|_{\mathcal{H}_t} \\ &\quad + \left\| (T_\nu + \lambda I)^{\frac{1}{2}} h_\lambda(T_\delta) f_2 \right\|_{\mathcal{H}_t} \\ &\triangleq J_1 + J_2. \end{aligned}$$

We consider term J_2 first. Since g_λ has qualification $\xi \geq 1$,

$$(t + \lambda)^\xi h_\lambda(t) \leq 2^{\xi-1} \left(t^\xi h_\lambda(t) + \lambda^\xi h_\lambda(t) \right) \leq 2^\xi \lambda^\xi. \quad (5.18)$$

Hence

$$\begin{aligned} J_2 &\leq \left\| (T_\nu + \lambda I)^{\frac{1}{2}} (T_\delta + \lambda I)^{-\frac{1}{2}} \right\|_{\mathcal{B}(\mathcal{H}_t)} \\ &\quad \cdot \left\| (T_\delta + \lambda I)^{\frac{1}{2}} h_\lambda(T_\delta) (T_\delta + \lambda I)^{\xi-\frac{1}{2}} \right\|_{\mathcal{B}(\mathcal{H}_t)} \cdot \left\| (T_\delta + \lambda I)^{\frac{1}{2}-\xi} f_2 \right\|_{\mathcal{H}_t}, \end{aligned}$$

where the first term above has been bounded in (5.6) and the second term above is bounded

by above calculation (5.18). For the third term, we have

$$\begin{aligned}
\left\| (T_\delta + \lambda I)^{\frac{1}{2}-\xi} f_2 \right\|_{\mathcal{H}_t} &= \left\| (T_\delta + \lambda I)^{\frac{1}{2}-\xi} g_\lambda(\tilde{T}_\delta) g_D^T \right\|_{\mathcal{H}_t} \\
&= \left\| \sum_{k=1}^q (\lambda + \lambda_k)^{\frac{1}{2}-\xi} g_\lambda(\tilde{\lambda}_k) \langle g_D, \phi_k \rangle_{\mathcal{H}_t} \phi_k \right\|_{\mathcal{H}_t} \\
&= \left(\sum_{k=1}^q (\lambda + \lambda_k)^{1-2\xi} g_\lambda(\tilde{\lambda}_k)^2 |\langle g_D, \phi_k \rangle_{\mathcal{H}_t}|^2 \right)^{\frac{1}{2}} \\
&\leq \left(\sum_{k=1}^q \lambda_k^{1-2\xi} \tilde{\lambda}_k^{-2} |\langle g_D, \phi_k \rangle_{\mathcal{H}_t}|^2 \right)^{\frac{1}{2}}.
\end{aligned}$$

Since (2.31) and (3.3) yields

$$|\tilde{\lambda}_k - \lambda_k| \lesssim \frac{1}{K} + \epsilon^{\frac{1}{4}},$$

whose convergence is independent of m . Therefore, the above term can be bounded as

$$\begin{aligned}
\left\| (T_\delta + \lambda I)^{\frac{1}{2}-\xi} f_2 \right\|_{\mathcal{H}_t} &\lesssim \left(\sum_{k=1}^q \lambda_k^{1-2\xi} \lambda_k^{-2} |\langle g_D, \phi_k \rangle_{\mathcal{H}_t}|^2 \right)^{\frac{1}{2}} \\
&\leq \lambda_q^{-\frac{1+2\xi}{2}} \left(\sum_{k=1}^q |\langle g_D, \phi_k \rangle_{\mathcal{H}_t}|^2 \right)^{\frac{1}{2}} \\
&\lesssim m^{\frac{1}{2r+1} \cdot \frac{1+2\xi}{2}},
\end{aligned}$$

where the last inequality follows from the definition of g_D as provided in (2.23), in conjunction with the boundedness condition and the lower bound result (D.4) on λ_q . Combining the above yields

$$\begin{aligned}
J_2 &\lesssim \lambda^\xi \cdot \lambda_q^{-\frac{1+2\xi}{2}} \\
&\lesssim \left(\frac{(\log m)^{\frac{d}{2}}}{m} \right)^{\frac{\xi}{2}} \cdot m^{\frac{1}{2r+1} \cdot \frac{1+2\xi}{2}} \\
&\lesssim m^{-\frac{\xi}{2} + \frac{1}{2r+1}(\xi + \frac{1}{2})} \cdot (\log m)^{\frac{d\xi}{4}}.
\end{aligned} \tag{5.19}$$

Note that $-\frac{\xi}{2} + \frac{1}{2r+1}(\xi + \frac{1}{2}) = -\frac{1}{2r+1}((r - \frac{1}{2})\xi - \frac{1}{2}) < 0$ for $\xi \geq 1$ and $r > 1$. Then we return to term J_1 . Notice that

$$\begin{aligned}
J_1 &= \left\| (T_\nu + \lambda I)^{\frac{1}{2}} g_\lambda(T_\delta) (g_D^T - T_\delta g_\lambda(\tilde{T}_\delta) g_D^T) \right\|_{\mathcal{H}_t} \\
&= \left\| (T_\nu + \lambda I)^{\frac{1}{2}} g_\lambda(T_\delta) \left(I - T_\delta g_\lambda(\tilde{T}_\delta) \right) g_D^T \right\|_{\mathcal{H}_t} \\
&\leq \left\| (T_\nu + \lambda I)^{\frac{1}{2}} (T_\delta + \lambda I)^{-\frac{1}{2}} \right\|_{\mathcal{B}(\mathcal{H}_t)} \cdot \left\| (T_\delta + \lambda I)^{\frac{1}{2}} g_\lambda(T_\delta) (T_\delta + \lambda I)^{\frac{1}{2}} \right\|_{\mathcal{B}(\mathcal{H}_t)} \\
&\quad \cdot \left\| (T_\delta + \lambda I)^{-\frac{1}{2}} \left(I - T_\delta g_\lambda(\tilde{T}_\delta) \right) g_D^T \right\|_{\mathcal{H}_t},
\end{aligned}$$

with the first and the second terms already bounded in (5.6) and (5.7). For the remaining term, since

$$\begin{aligned} I - T_\delta g_\lambda(\tilde{T}_\delta) &= I - \tilde{T}_\delta g_\lambda(\tilde{T}_\delta) + \tilde{T}_\delta g_\lambda(\tilde{T}_\delta) - T_\delta g_\lambda(\tilde{T}_\delta) \\ &= h_\lambda(\tilde{T}_\delta) + (\tilde{T}_\delta - T_\delta) g_\lambda(\tilde{T}_\delta), \end{aligned}$$

a further decomposition it derived as

$$\begin{aligned} \left\| (T_\delta + \lambda I)^{-\frac{1}{2}} \left(I - T_\delta g_\lambda(\tilde{T}_\delta) \right) g_D^T \right\|_{\mathcal{H}_t} &\leq \left\| (T_\delta + \lambda I)^{-\frac{1}{2}} h_\lambda(\tilde{T}_\delta) g_D^T \right\|_{\mathcal{H}_t} \\ &\quad + \left\| (T_\delta + \lambda I)^{-\frac{1}{2}} (\tilde{T}_\delta - T_\delta) g_\lambda(\tilde{T}_\delta) g_D^T \right\|_{\mathcal{H}_t} \\ &\triangleq L_1 + L_2. \end{aligned}$$

For L_1 we have

$$L_1 \leq \left\| (T_\delta + \lambda I)^{-\frac{1}{2}} (\tilde{T}_\delta + \lambda I)^{\frac{1}{2}} \right\|_{\mathcal{B}(\mathcal{H}_t)} \cdot \left\| (\tilde{T}_\delta + \lambda I)^{-\frac{1}{2}} h_\lambda(\tilde{T}_\delta) g_D^T \right\|_{\mathcal{H}_t}.$$

It's remarkable that our analysis of the operator norm can be specifically confined to the subspace $L_q = \text{Span}\{\phi_k : 1 \leq k \leq q\}$, given that $g_D^T \in L_q$ and all operators under consideration exhibit L_q -invariance. Therefore,

$$\begin{aligned} \left\| (T_\delta + \lambda I)^{-\frac{1}{2}} (\tilde{T}_\delta + \lambda I)^{\frac{1}{2}} \right\|_{\mathcal{B}(L_q)}^2 &= \sup_{1 \leq k \leq q} \frac{\lambda_k + \lambda}{\tilde{\lambda}_k + \lambda} \\ &= 1 + \sup_{1 \leq k \leq q} \frac{\lambda_k - \tilde{\lambda}_k}{\tilde{\lambda}_k + \lambda} \\ &\leq 1 + \tilde{\lambda}_q^{-1} \cdot \sup_{1 \leq k \leq q} |\lambda_k - \tilde{\lambda}_k| \\ &\lesssim 1 + m^{\frac{1}{2r+1}} \left(\frac{1}{K} + \epsilon^{\frac{1}{4}} \right) \lesssim 2. \end{aligned}$$

For the remaining \mathcal{H}_t -norm, a similar approach as in the upper bound analysis of J_2 yields

$$\begin{aligned} \left\| (\tilde{T}_\delta + \lambda I)^{-\frac{1}{2}} h_\lambda(\tilde{T}_\delta) g_D^T \right\|_{\mathcal{H}_t} &\leq \left\| (\tilde{T}_\delta + \lambda I)^{-\frac{1}{2}} h_\lambda(\tilde{T}_\delta) (\tilde{T}_\delta + \lambda I)^{\frac{1}{2} + \xi} \right\|_{\mathcal{B}(\mathcal{H}_t)} \\ &\quad \cdot \left\| (\tilde{T}_\delta + \lambda I)^{-\frac{1}{2} - \xi} g_D^T \right\|_{\mathcal{H}_t}, \end{aligned}$$

with the first term also bounded by calculation (5.18). For the second term, we have

$$\begin{aligned} \left\| (\tilde{T}_\delta + \lambda I)^{-\frac{1}{2} - \xi} g_D^T \right\|_{\mathcal{H}_t} &= \left(\sum_{k=1}^q (\lambda + \tilde{\lambda}_k)^{-1 - 2\xi} |\langle g_D, \phi_k \rangle_{\mathcal{H}_t}|^2 \right)^{\frac{1}{2}} \\ &\lesssim \lambda_q^{-\frac{1+2\xi}{2}} \left(\sum_{k=1}^q |\langle g_D, \phi_k \rangle_{\mathcal{H}_t}|^2 \right)^{\frac{1}{2}} \\ &\lesssim m^{\frac{1}{2r+1}} \cdot \lambda_q^{-\frac{1+2\xi}{2}}. \end{aligned}$$

Combining the above yields

$$L_1 \lesssim \lambda^\xi \lambda_q^{-\frac{1+2\xi}{2}} \lesssim m^{-\frac{\xi}{2} + \frac{1}{2r+1}(\xi + \frac{1}{2})} \cdot (\log m)^{\frac{d\xi}{4}}. \quad (5.20)$$

Now we consider L_2 . It can be decomposed as

$$L_2 \leq \left\| (T_\delta + \lambda I)^{-\frac{1}{2}} \right\|_{\mathcal{B}(\mathcal{H}_t)} \cdot \left\| \tilde{T}_\delta - T_\delta \right\|_{\mathcal{B}(\mathcal{H}_t)} \cdot \left\| g_\lambda(\tilde{T}_\delta) g_D^T \right\|_{\mathcal{H}_t}.$$

Similarly, we can restrict all operator norms to subspace L_q . Therefore, we have

$$\left\| (T_\delta + \lambda I)^{-\frac{1}{2}} \right\|_{\mathcal{B}(L_q)} = \sup_{1 \leq k \leq q} \frac{1}{\sqrt{\lambda_k + \lambda}} \leq \lambda_q^{-\frac{1}{2}} \lesssim m^{\frac{1}{2r+1} \cdot \frac{1}{2}},$$

and

$$\left\| \tilde{T}_\delta - T_\delta \right\|_{\mathcal{B}(L_q)} = \sup_{1 \leq k \leq q} |\tilde{\lambda}_k - \lambda_k| \lesssim \frac{1}{K} + \epsilon^{\frac{1}{4}}.$$

For the third term of L_2 , a direct calculation shows

$$\begin{aligned} \left\| g_\lambda(\tilde{T}_\delta) g_D^T \right\|_{\mathcal{H}_t} &= \left(\sum_{k=1}^q g_\lambda(\tilde{\lambda}_k)^2 |\langle g_D, \phi_k \rangle_{\mathcal{H}_t}|^2 \right)^{\frac{1}{2}} \\ &\lesssim \lambda_q^{-1} \left(\sum_{k=1}^q |\langle g_D, \phi_k \rangle_{\mathcal{H}_t}|^2 \right)^{\frac{1}{2}} \\ &\lesssim m^{\frac{1}{2r+1}}. \end{aligned}$$

Combining the above yields

$$L_2 \lesssim m^{\frac{1}{2r+1} \cdot \frac{3}{2}} \left(\frac{1}{K} + \epsilon^{\frac{1}{4}} \right). \quad (5.21)$$

By combining (5.20) and (5.21) with the previous upper bounds (5.6) and (5.7), we derive that

$$J_1 \lesssim m^{-\frac{\xi}{2} + \frac{1}{2r+1}(\xi + \frac{1}{2})} \cdot (\log m)^{\frac{d\xi}{4}} + m^{\frac{1}{2r+1} \cdot \frac{3}{2}} \left(\frac{1}{K} + \epsilon^{\frac{1}{4}} \right). \quad (5.22)$$

Therefore, a combination of (5.19) and (5.22) with previous upper bounds (5.4) results in

$$\begin{aligned} \left\| \left(g_\lambda(T_\delta) - g_\lambda(\tilde{T}_\delta) \right) g_D^T \right\|_\alpha &\lesssim \lambda^{-\frac{\alpha}{2}} \left(m^{-\frac{\xi}{2} + \frac{1}{2r+1}(\xi + \frac{1}{2})} \cdot (\log m)^{\frac{d\xi}{4}} + m^{\frac{1}{2r+1} \cdot \frac{3}{2}} \left(\frac{1}{K} + \epsilon^{\frac{1}{4}} \right) \right) \\ &\lesssim m^{-\frac{\xi}{2} + \frac{1}{2r+1}(\xi + \frac{1}{2}) + \frac{\alpha}{4}} \cdot (\log m)^{\frac{d\xi}{4} - \frac{d\alpha}{8}} \\ &\quad + m^{\frac{1}{2r+1} \cdot \frac{3}{2} + \frac{\alpha}{4}} \cdot (\log m)^{-\frac{d\alpha}{8}} \cdot \left(\frac{1}{K} + \epsilon^{\frac{1}{4}} \right). \end{aligned}$$

Finally, the embedding property $\mathcal{H}_t^\alpha \hookrightarrow L^\infty(\nu)$ yields

$$I_1 \lesssim m^{-\frac{\xi}{2} + \frac{1}{2r+1}(\xi + \frac{1}{2}) + \frac{\alpha}{4}} \cdot (\log m)^{\frac{d\xi}{4} - \frac{d\alpha}{8}} + m^{\frac{1}{2r+1} \cdot \frac{3}{2} + \frac{\alpha}{4}} \cdot (\log m)^{-\frac{d\alpha}{8}} \cdot \left(\frac{1}{K} + \epsilon^{\frac{1}{4}} \right),$$

which valid for all $\alpha > 0$. This completes the proof. \square

We now focus our attention on term I_2 , the upper bound result of which is summarized in the following Lemma 7.

Lemma 7. *Suppose that Assumption 1 and Assumption 2 hold. Suppose that the conditions (2.38) holds with m sufficiently large, $N > K \gg m$ sufficiently large and ϵ sufficiently small. We choose q as in (3.2). Denote E_1 the event given in Theorem 1 and E_2 the good event proposed in Theorem 3. Then, on $E_1 \cap E_2$, for any $1 \leq j \leq N$, it holds*

$$I_2 \leq K'_2 m^{\frac{2r+4}{2r+1}} (\log m)^{\frac{d}{2}} \cdot \left(\frac{1}{K} + \epsilon^{\frac{1}{4}} \right),$$

where K'_2 is a constant independent of m, K, N, ϵ .

Proof. We first decompose I_2 as

$$\begin{aligned} I_2 &= \left| \sum_{k=1}^q g_\lambda(\tilde{\lambda}_k) \left(\langle g_D, \phi_k \rangle_{\mathcal{H}_t} \phi_k(x_j) - \tilde{g}_{D,k} \tilde{\phi}_k(j) \right) \right| \\ &\leq \sum_{k=1}^q \left| g_\lambda(\tilde{\lambda}_k) \right| \cdot |\langle g_D, \phi_k \rangle_{\mathcal{H}_t} - \tilde{g}_{D,k}| \cdot |\phi_k(x_j)| \\ &\quad + \sum_{k=1}^q \left| g_\lambda(\tilde{\lambda}_k) \right| \cdot |\tilde{g}_{D,k}| \cdot \left| \phi_k(x_j) - \tilde{\phi}_k(j) \right|. \end{aligned}$$

Notice that

$$\left| g_\lambda(\tilde{\lambda}_k) \right| \leq \tilde{\lambda}_k^{-1} \lesssim m^{\frac{1}{2r+1}},$$

which is already established in (D.4). Recall the definition (3.7) of $\tilde{g}_{D,k}$, combining with the reproducing property, we have

$$\begin{aligned} |\langle g_D, \phi_k \rangle_{\mathcal{H}_t} - \tilde{g}_{D,k}| &= \left| \frac{1}{m} \sum_{i=1}^m y_i \phi_k(x_i) - \frac{1}{m} \sum_{i=1}^m y_i \tilde{\phi}_k(i) \right| \\ &\leq \frac{1}{m} \sum_{i=1}^m |y_i| \cdot |\phi_k(x_i) - \tilde{\phi}_k(i)|. \end{aligned}$$

By the eigenfunction estimation result (3.6), we have

$$|\langle g_D, \phi_k \rangle_{\mathcal{H}_t} - \tilde{g}_{D,k}| \lesssim m^{\frac{r+2}{2r+1}} \left(\frac{1}{K} + \epsilon^{\frac{1}{4}} \right).$$

From the definition of ϕ_k as in (2.31), we have

$$|\phi_k(x_j)| = \left| \frac{1}{\sqrt{m\hat{\lambda}_k}} \sum_{i=1}^m \hat{u}_k(i) H_t(x_i, x_j) \right| \lesssim m^{\frac{r+1}{2r+1}}, \quad (5.23)$$

where the inequality follows from (D.2), that \hat{u}_k is a unit vector, and the boundedness condition on heat kernel. Combining the above yields

$$\begin{aligned} \sum_{k=1}^q \left| g_\lambda(\tilde{\lambda}_k) \right| \cdot |\langle g_D, \phi_k \rangle_{\mathcal{H}_t} - \tilde{g}_{D,k}| \cdot |\phi_k(x_j)| &\lesssim q \cdot m^{\frac{3}{2r+1}+1} \left(\frac{1}{K} + \epsilon^{\frac{1}{4}} \right) \\ &\lesssim m^{\frac{3}{2r+1}+1} (\log m)^{\frac{d}{2}} \cdot \left(\frac{1}{K} + \epsilon^{\frac{1}{4}} \right). \end{aligned} \quad (5.24)$$

For the second term, we have

$$|\tilde{g}_{D,k}| \leq |\langle g_D, \phi_k \rangle_{\mathcal{H}_t}| + |\langle g_D, \phi_k \rangle_{\mathcal{H}_t} - \tilde{g}_{D,k}|.$$

Notice that

$$|\langle g_D, \phi_k \rangle_{\mathcal{H}_t}| \leq \|g_D\|_{\mathcal{H}_t} \cdot \|\phi_k\|_{\mathcal{H}_t} \leq M\kappa^2, \quad (5.25)$$

since ϕ_k an orthonormal base of \mathcal{H}_t and $\|H_t(x_i, \cdot)\|_{\mathcal{H}_t} = H_t(x_i, x_i) \leq \kappa^2$. Therefore,

$$|\tilde{g}_{D,k}| \lesssim M\kappa^2 + m^{\frac{r+2}{2r+1}} \left(\frac{1}{K} + \epsilon^{\frac{1}{4}} \right) \lesssim M\kappa^2.$$

Combining this upper bound with (3.6) and (D.4), we derive that

$$\begin{aligned} \sum_{k=1}^q \left| g_\lambda(\tilde{\lambda}_k) \right| \cdot |\tilde{g}_{D,k}| \cdot \left| \phi_k(x_j) - \tilde{\phi}_k(j) \right| &\lesssim q \cdot m^{\frac{r+3}{2r+1}} \left(\frac{1}{K} + \epsilon^{\frac{1}{4}} \right) \\ &\lesssim m^{\frac{r+3}{2r+1}} (\log m)^{\frac{d}{2}} \cdot \left(\frac{1}{K} + \epsilon^{\frac{1}{4}} \right). \end{aligned} \quad (5.26)$$

Finally, combining (5.24) and (5.26), we derive that

$$I_2 \lesssim m^{\frac{3}{2r+1}+1} (\log m)^{\frac{d}{2}} \cdot \left(\frac{1}{K} + \epsilon^{\frac{1}{4}} \right),$$

which completes the proof. \square

Combining Lemma 6 and Lemma 7, we finally derive the following Theorem 6.

Theorem 6. *Suppose that Assumption 1, Assumption 2, and Assumption 3 hold. Suppose that the conditions (2.38) holds with m sufficiently large, $N > K \gg m$ sufficiently large and ϵ sufficiently small. We choose q, λ as in (3.2) and (3.11) separately. Denote E_1 the event given in Theorem 1, E_2 the event given in Theorem 3, and E_3 the event given in Theorem 5. Then, for any $0 < \alpha \leq 1$ and $1 \leq j \leq N$, on $E_1 \cap E_2 \cap E_3$, it holds*

$$|f_{D,\lambda}^T(x_j) - \tilde{f}_{D,\lambda}(j)| \leq K_a \left(m^{-\frac{\xi}{2} + \frac{\xi+1}{2r+1} + \frac{\alpha}{4}} \cdot (\log m)^{\frac{d\xi}{4} - \frac{d\alpha}{8}} + m^{\frac{3}{2r+1}+1} (\log m)^{\frac{d}{2}} \cdot \left(\frac{1}{K} + \epsilon^{\frac{1}{4}} \right) \right)$$

with K_a a constant independent of $m, K, N, \epsilon, \alpha$.

5.3 Proof of Theorem 4

Proof of Theorem 4. Since for any $m+1 \leq j \leq m+n$,

$$\begin{aligned} |\tilde{f}_{D,\lambda}(j) - f^*(x_j)| &\leq |\tilde{f}_{D,\lambda}(j) - f_{D,\lambda}^T(x_j)| + |f_{D,\lambda}^T(x_j) - f^*(x_j)| \\ &\leq |\tilde{f}_{D,\lambda}(j) - f_{D,\lambda}^T(x_j)| + \|f_{D,\lambda}^T - f^*\|_\infty, \end{aligned}$$

a direct combination of Theorem 5 and Theorem 6 yields

$$\begin{aligned}
|\tilde{f}_{D,\lambda}(j) - f^*(x_j)| &\leq K_t m^{-\frac{C_{low}}{C_{up}} \cdot \frac{1}{2} + \frac{\alpha}{4}} (\log m)^{\frac{1}{2} + \frac{d}{4} - \frac{\alpha d}{8}} \\
&\quad + K_a \left(m^{-\frac{\xi}{2} + \frac{\xi + \frac{1}{2}}{2r+1} + \frac{\alpha}{4}} \cdot (\log m)^{\frac{d\xi}{4} - \frac{d\alpha}{8}} + m^{\frac{3}{2r+1} + 1} (\log m)^{\frac{d}{2}} \cdot \left(\frac{1}{K} + \epsilon^{\frac{1}{4}} \right) \right) \\
&\leq C m^{-\theta_1} \cdot (\log m)^{\theta_2} + C' m^{\frac{3}{2r+1} + 1} (\log m)^{\frac{d}{2}} \cdot \left(\frac{1}{K} + \epsilon^{\frac{1}{4}} \right).
\end{aligned}$$

Here, θ_1 and θ_2 are as defined in (3.13), and C, C' are constants independent of $m, K, N, \epsilon, \alpha$. This completes the proof. \square

References

- [1] Frank Bauer, Sergei Pereverzev, and Lorenzo Rosasco. On regularization algorithms in learning theory. *Journal of Complexity*, 23(1):52–72, 2007.
- [2] Mikhail Belkin and Partha Niyogi. Laplacian eigenmaps for dimensionality reduction and data representation. *Neural Computation*, 15(6):1373–1396, 2003.
- [3] Richard E. Bellman. *Adaptive Control Processes: A Guided Tour*. Princeton University Press, Princeton, 1961.
- [4] Pierre Bérard, Gérard Besson, and Sylvain Gallot. Embedding Riemannian manifolds by their heat kernel. *Geometric & Functional Analysis GAFA*, 4:373–398, 1994.
- [5] Gilles Blanchard and Nicole Mücke. Optimal rates for regularization of statistical inverse learning problems. *Foundations of Computational Mathematics*, 18(4):971–1013, 2018.
- [6] Jonathan M Borwein and O-Yeat Chan. Uniform bounds for the incomplete complementary Gamma function. *Mathematical Inequalities and Applications*, 12:115–121, 2009.
- [7] Mikio L Braun. Accurate error bounds for the eigenvalues of the kernel matrix. *The Journal of Machine Learning Research*, 7:2303–2328, 2006.
- [8] Roberto Calandra, Jan Peters, Carl Edward Rasmussen, and Marc Peter Deisenroth. Manifold Gaussian processes for regression. *2016 International Joint Conference on Neural Networks (IJCNN)*, pages 3338–3345, 2014.
- [9] Jeff Calder, Nicolas Garcia Trillos, and Marta Lewicka. Lipschitz regularity of graph Laplacians on random data clouds. *SIAM Journal on Mathematical Analysis*, 54(1):1169–1222, 2022.
- [10] Jeff Calder and Nicolas Garcia Trillos. Improved spectral convergence rates for graph Laplacians on ϵ -graphs and k-NN graphs. *Applied and Computational Harmonic Analysis*, 60:123–175, 2022.
- [11] Andrea Caponnetto and Ernesto De Vito. Optimal rates for the regularized least-squares algorithm. *Foundations of Computational Mathematics*, 7:331–368, 2007.
- [12] Andrea Caponnetto and Yuan Yao. Cross-validation based adaptation for regularization operators in learning theory. *Analysis and Applications*, 8(02):161–183, 2010.

- [13] Gunnar Carlsson, Tigran Ishkhanov, Vin De Silva, and Afra Zomorodian. On the local behavior of spaces of natural images. *International Journal of Computer Vision*, 76:1–12, 2008.
- [14] Alain Celisse and Martin Wahl. Analyzing the discrepancy principle for kernelized spectral filter learning algorithms. *The Journal of Machine Learning Research*, 22(1):3498–3556, 2021.
- [15] Isaac Chavel. *Eigenvalues in Riemannian Geometry*. Academic Press, 1984.
- [16] Xiuyuan Cheng and Nan Wu. Eigen-convergence of Gaussian kernelized graph Laplacian by manifold heat interpolation. *Applied and Computational Harmonic Analysis*, 61:132–190, 2022.
- [17] Yasuko Chikuse. *Statistics on Special Manifolds*, volume 174. Springer Science & Business Media, 2012.
- [18] Ronald R Coifman and Stéphane Lafon. Diffusion maps. *Applied and Computational Harmonic Analysis*, 21(1):5–30, 2006.
- [19] Felipe Cucker and Steve Smale. On the mathematical foundations of learning. *Bulletin of the American Mathematical Society*, 39(1):1–49, 2002.
- [20] Edward Brian Davies. *Heat Kernels and Spectral Theory*. Number 92. Cambridge University Press, 1989.
- [21] Chandler Davis and William Morton Kahan. The rotation of eigenvectors by a perturbation. III. *SIAM Journal on Numerical Analysis*, 7(1):1–46, 1970.
- [22] Ernesto De Vito, Nicole Mücke, and Lorenzo Rosasco. Reproducing kernel Hilbert spaces on manifolds: Sobolev and diffusion spaces. *Analysis and Applications*, 19(03):363–396, 2021.
- [23] David B Dunson, Hau-Tieng Wu, and Nan Wu. Diffusion based Gaussian process regression via heat kernel reconstruction. *arXiv preprint arXiv:1912.05680*, 2019.
- [24] David B Dunson, Hau-Tieng Wu, and Nan Wu. Spectral convergence of graph Laplacian and heat kernel reconstruction in L^∞ from random samples. *Applied and Computational Harmonic Analysis*, 55:282–336, 2021.
- [25] Simon Fischer and Ingo Steinwart. Sobolev norm learning rates for regularized least-squares algorithms. *The Journal of Machine Learning Research*, 21(1):8464–8501, 2020.
- [26] Joachim Frank. *Three-dimensional Electron Microscopy of Macromolecular Assemblies: Visualization of Biological Molecules in Their Native State*. Oxford University Press, 2006.
- [27] Joel N Franklin. *Matrix Theory*. Courier Corporation, 2012.
- [28] L Lo Gerfo, Lorenzo Rosasco, Francesca Odone, E De Vito, and Alessandro Verri. Spectral algorithms for supervised learning. *Neural Computation*, 20(7):1873–1897, 2008.
- [29] Alexander Grigoryan. *Heat Kernel and Analysis on Manifolds*, volume 47. American Mathematical Soc., 2009.

- [30] Rajarshi Guhaniyogi and David B Dunson. Compressed Gaussian process for manifold regression. *The Journal of Machine Learning Research*, 17(1):2472–2497, 2016.
- [31] Xin Guo and Ding-Xuan Zhou. An empirical feature-based learning algorithm producing sparse approximations. *Applied and Computational Harmonic Analysis*, 32(3):389–400, 2012.
- [32] Zheng-Chu Guo, Dao-Hong Xiang, Xin Guo, and Ding-Xuan Zhou. Thresholded spectral algorithms for sparse approximations. *Analysis and Applications*, 15(03):433–455, 2017.
- [33] László Györfi, Michael Kohler, Adam Krzyzak, and Harro Walk. *A Distribution-free Theory of Nonparametric Regression*, volume 1. Springer, 2002.
- [34] Thomas Hamm and Ingo Steinwart. Adaptive learning rates for support vector machines working on data with low intrinsic dimension. *The Annals of Statistics*, 49(6):3153–3180, 2021.
- [35] Emmanuel Hebey. *Nonlinear Analysis on Manifolds: Sobolev Spaces and Inequalities: Sobolev Spaces and Inequalities*, volume 5. American Mathematical Soc., 2000.
- [36] Lars Hörmander. The spectral function of an elliptic operator. In *Mathematics Past and Present Fourier Integral Operators*, pages 217–242. Springer, 1968.
- [37] Elton P Hsu. *Stochastic Analysis on Manifolds*. Number 38. American Mathematical Soc., 2002.
- [38] Kwang-Sung Jun, Ashok Cutkosky, and Francesco Orabona. Kernel truncated randomized ridge regression: Optimal rates and low noise acceleration. *Advances in Neural Information Processing Systems*, 32, 2019.
- [39] Vladimir Koltchinskii and Evarist Giné. Random matrix approximation of spectra of integral operators. *Bernoulli*, pages 113–167, 2000.
- [40] John M Lee. *Introduction to Riemannian manifolds*, volume 2. Springer, 2018.
- [41] Peter Li and Shing-Tung Yau. On the schrödinger equation and the eigenvalue problem. *Communications in Mathematical Physics*, 88(3):309–318, 1983.
- [42] Junhong Lin and Volkan Cevher. Optimal distributed learning with multi-pass stochastic gradient methods. In *International Conference on Machine Learning*, pages 3092–3101. PMLR, 2018.
- [43] Junhong Lin, Alessandro Rudi, Lorenzo Rosasco, and Volkan Cevher. Optimal rates for spectral algorithms with least-squares regression over Hilbert spaces. *Applied and Computational Harmonic Analysis*, 48(3):868–890, 2020.
- [44] Andrew McRae, Justin Romberg, and Mark Davenport. Sample complexity and effective dimension for regression on manifolds. *Advances in Neural Information Processing Systems*, 33:12993–13004, 2020.
- [45] Stefano Melacci and Mikhail Belkin. Laplacian support vector machines trained in the primal. *The Journal of Machine Learning Research*, 12(3), 2011.
- [46] Beresford N Parlett. *The Symmetric Eigenvalue Problem*. SIAM, 1998.

- [47] Peter Petersen. *Riemannian Geometry*, volume 171. Springer, 2006.
- [48] Loucas Pillaud-Vivien, Alessandro Rudi, and Francis Bach. Statistical optimality of stochastic gradient descent on hard learning problems through multiple passes. *Advances in Neural Information Processing Systems*, 31, 2018.
- [49] Michael Reed and Barry Simon. *Methods of Modern Mathematical Physics. vol. 1. Functional analysis*. Academic New York, 1980.
- [50] Michael Reed, Barry Simon, and SM Reed. *Methods of Modern Mathematical Physics: Fourier Analysis, Self-Adjointness*. World Book Publishing Company, 2003.
- [51] Lorenzo Rosasco, Ernesto De Vito, and Alessandro Verri. Spectral methods for regularization in learning theory. *DISI, Universita degli Studi di Genova, Italy, Technical Report DISI-TR-05-18*, 2005.
- [52] Takashi Sakai. *Riemannian Geometry*, volume 149. American Mathematical Soc., 1996.
- [53] Bernhard Schölkopf and Alexander J Smola. *Learning with Kernels: Support Vector Machines, Regularization, Optimization, and Beyond*. MIT press, 2002.
- [54] Amit Singer. From graph to manifold Laplacian: The convergence rate. *Applied and Computational Harmonic Analysis*, 21(1):128–134, 2006.
- [55] Ingo Steinwart and Andreas Christmann. *Support Vector Machines*. Springer Science & Business Media, 2008.
- [56] Ingo Steinwart, Don R Hush, and Clint Scovel. Optimal rates for regularized least squares regression. In *Conference on Learning Theory*, pages 79–93, 2009.
- [57] Robert S Strichartz. Analysis of the Laplacian on the complete riemannian manifold. *Journal of Functional Analysis*, 52(1):48–79, 1983.
- [58] Hans Triebel. *Theory of Function Spaces II*. Birkhäuser Basel, 2010.
- [59] Ulrike Von Luxburg. A tutorial on spectral clustering. *Statistics and Computing*, 17:395–416, 2007.
- [60] Martin J Wainwright. *High-dimensional Statistics: A Non-asymptotic Viewpoint*, volume 48. Cambridge University Press, 2019.
- [61] Hermann Weyl. Das asymptotische verteilungsgesetz der eigenwerte linearer partieller differentialgleichungen (mit einer anwendung auf die theorie der hohlraumstrahlung). *Mathematische Annalen*, 71(4):441–479, 1912.
- [62] Weichun Xia and Lei Shi. Spectral algorithms on manifolds through diffusion. *arXiv preprint arXiv:2403.03669*, 2024.
- [63] Haobo Zhang, Yicheng Li, and Qian Lin. On the optimality of misspecified spectral algorithms. *The Journal of Machine Learning Research*, 25(188):1–50, 2024.

A Proof of Theorem 1

Proof. Based on the eigen-convergence results presented in [16], we first re-normalize the eigenvector \tilde{v}_k as $\tilde{u}_k = \frac{1}{\sqrt{pN}}\tilde{v}_k$ to establish an orthonormal basis of \mathbb{R}^N . Therefore, with probability at least $1 - c_1N^{-8}$, for each $1 \leq k \leq K$, the following approximation holds:

$$|\tilde{\mu}_k - \mu_k| \lesssim \left(\frac{\log N}{N}\right)^{\frac{1}{\frac{d}{2}+2}}, \quad (\text{A.1})$$

$$\left\| \tilde{u}_k - \alpha_k \rho_X \left(\frac{1}{\sqrt{pN}} \psi_k \right) \right\|_{l^2} \lesssim \left(\frac{\log N}{N} \right)^{\frac{1}{d+4}}. \quad (\text{A.2})$$

Here, $|\alpha_k| = 1$ represents the direction, and $\|\cdot\|_{l^2}$ denotes the standard Euclidean 2-norm on \mathbb{R}^N . We may assume without loss of generality that $\alpha_k = 1$ for all $1 \leq k \leq K$. Our targeted eigenvalue upper bound (2.35) directly follows from (A.1). The focus then shifts to translating the l^2 -norm bound (A.2) to our targeted l^∞ -norm bound (2.36). This translation involves defining several normalized norms on \mathbb{R}^N as

$$\begin{aligned} \|u\|_2^2 &\triangleq \frac{1}{N} \sum_{i=1}^N u_i^2, \\ \|u\|_1 &\triangleq \frac{1}{N} \sum_{i=1}^N |u_i|, \end{aligned}$$

leading to the relationship

$$\begin{aligned} \|\tilde{v}_k - \rho_X(\psi_k)\|_2 &= \frac{1}{\sqrt{N}} \|\tilde{u}_k - \rho_X(\psi_k)\|_{l^2} \\ &= \sqrt{p} \left\| \tilde{u}_k - \rho_X \left(\frac{1}{\sqrt{pN}} \psi_k \right) \right\|_{l^2} \lesssim \left(\frac{\log N}{N} \right)^{\frac{1}{d+4}}. \end{aligned} \quad (\text{A.3})$$

Given the Gaussian kernel basis for our un-normalized graph Laplacian L_{un} , we further achieve a point-wise convergence rate on sample points with a probability of at least $1 - 2N^{-9}$ as

$$\|L_{un}\rho_X(f) - \rho_X(\Delta f)\|_\infty \lesssim \left(\frac{\log N}{N} \right)^{\frac{1}{d+4}}. \quad (\text{A.4})$$

Such a result could also be found in [10]. Now we introduce another un-normalized graph Laplacian L_{un}^I , constructed with the indicator kernel K_I , defined as

$$K_I(x, z) = \epsilon^{-\frac{d}{2}} \mathbb{1}_{\{\|x-z\| \leq \sqrt{\epsilon}\}}.$$

Let $\varepsilon_k = \tilde{v}_k - \rho_X(\psi_k)$, and we assume $\varepsilon_k \neq 0$ (Otherwise, there is nothing to be proved). We further define

$$\lambda_k = \frac{\|L_{un}^I \varepsilon_k\|_\infty}{\|\varepsilon_k\|_\infty}. \quad (\text{A.5})$$

Therefore, we have

$$L_{un}^I \varepsilon_k = L_{un}^I (\tilde{v}_k - \rho_X(\psi_k))$$

$$= (L_{un}\tilde{v}_k - \rho_X(\Delta\psi_k)) + (L_{un}^I\tilde{v}_k - L_{un}\tilde{v}_k) + (\rho_X(\Delta\psi_k) - L_{un}^I(\rho_X(\psi_k))). \quad (\text{A.6})$$

For the first term in (A.6) we have

$$\begin{aligned} L_{un}\tilde{v}_k - \rho_X(\Delta\psi_k) &= \tilde{\mu}_k\tilde{v}_k - \rho_X(\mu_k\psi_k) \\ &= \tilde{\mu}_k(\tilde{v}_k - \rho_X(\psi_k)) + (\tilde{\mu}_k - \mu_k)\rho_X(\psi_k). \end{aligned}$$

Hence

$$\begin{aligned} \|L_{un}\tilde{v}_k - \rho_X(\Delta\psi_k)\|_\infty &\leq \tilde{\mu}_k\|\varepsilon_k\|_\infty + |\tilde{\mu}_k - \mu_k| \cdot \|\rho_X(\psi_k)\|_\infty \\ &\leq \tilde{\mu}_k\|\varepsilon_k\|_\infty + |\tilde{\mu}_k - \mu_k| \cdot \|\psi_k\|_{L^\infty(\mathcal{M})}. \end{aligned}$$

Since $\mu_k \leq \mu_K$ and K is a fixed constant, combining (2.7) and (A.1) we have

$$\|L_{un}\tilde{v}_k - \rho_X(\Delta\psi_k)\|_\infty \leq \tilde{\mu}_k\|\varepsilon_k\|_\infty + C \left(\frac{\log N}{N} \right)^{\frac{1}{\frac{d}{2}+2}}, \quad (\text{A.7})$$

where constant C is independent of N, ϵ . For the second term in (A.6) we have

$$\|L_{un}^I\tilde{v}_k - L_{un}\tilde{v}_k\|_\infty \leq \|L_{un}^I\tilde{v}_k - \rho_X(\Delta f_k)\|_\infty + \|L_{un}\tilde{v}_k - \rho_X(\Delta f_k)\|_\infty$$

with some function $f_k \in C^\infty(\mathcal{M})$ satisfying $\tilde{v}_k = \rho_X(f_k)$. For the un-normalized graph Laplacian L_{un}^I , a point-wise convergence result parallel to that of L_{un} as in (A.4) is also available, as shown in [10]:

$$\|L_{un}^I\rho_X(f) - \rho_X(\Delta f)\|_\infty \lesssim \left(\frac{\log N}{N} \right)^{\frac{1}{d+4}}. \quad (\text{A.8})$$

As a consequence, a combination of (A.4) and (A.8) yields

$$\|L_{un}^I\tilde{v}_k - L_{un}\tilde{v}_k\|_\infty \lesssim \left(\frac{\log N}{N} \right)^{\frac{1}{d+4}}. \quad (\text{A.9})$$

For the remained third term in (A.6), it follows directly from (A.8) that

$$\|\rho_X(\Delta\psi_k) - L_{un}^I(\rho_X(\psi_k))\|_\infty \lesssim \left(\frac{\log N}{N} \right)^{\frac{1}{d+4}}. \quad (\text{A.10})$$

Finally, by combining (A.7), (A.9), and (A.10) we have

$$\|L_{un}^I\varepsilon_k\|_\infty \leq \tilde{\mu}_k\|\varepsilon_k\|_\infty + C' \left(\frac{\log N}{N} \right)^{\frac{1}{d+4}},$$

where constant C' is independent of N, ϵ . Therefore, from definition (A.5) we have

$$\lambda_k \leq \tilde{\mu}_k + C' \frac{\left(\frac{\log N}{N} \right)^{\frac{1}{d+4}}}{\|\varepsilon_k\|_\infty}.$$

Now we consider two possible cases.

Case 1: $\lambda_k \geq \tilde{\mu}_k + 1$, which implies

$$\|\varepsilon_k\|_\infty \leq C' \left(\frac{\log N}{N} \right)^{\frac{1}{d+4}}.$$

Case 2: $\lambda_k < \tilde{\mu}_k + 1$. By exploiting techniques in [9] we can derive that, with probability at least $1 - c_2 N^{-8}$, it holds

$$\|\varepsilon_k\|_\infty \lesssim (\lambda_k + 1)^{d+1} \|\varepsilon_k\|_1.$$

A direct calculation using Cauchy-Schwarz inequality combined with (A.3) leads to

$$\|\varepsilon_k\|_\infty \lesssim (\tilde{\mu}_k + 2)^{d+1} \|\varepsilon_k\|_2 \lesssim \left(\frac{\log N}{N} \right)^{\frac{1}{d+4}},$$

where the last inequality also follows from the fact that $k \leq K$ and K is a fixed constant. Finally, combining above two cases yields the desired l^∞ upper bound

$$\|\varepsilon_k\|_\infty \lesssim \left(\frac{\log N}{N} \right)^{\frac{1}{d+4}}.$$

The proof is then finished. \square

B Proof of Theorem 2

Proof. For any $i, j \in \{1, \dots, N\}$, we divide the point-wise error into two parts

$$\begin{aligned} \left| H_t(x_i, x_j) - \tilde{H}_{t,K}(i, j) \right| &\leq \left| \sum_{k=1}^K (e^{-\tilde{\mu}_k t} \tilde{v}_k(i) \tilde{v}_k(j) - e^{-\mu_k t} \psi_k(x_i) \psi_k(x_j)) \right| \\ &\quad + \left| \sum_{k=K+1}^{\infty} e^{-\mu_k t} \psi_k(x_i) \psi_k(x_j) \right| \\ &\triangleq I_1 + I_2. \end{aligned}$$

Initially, we concentrate on the second term I_2 . An application of the Cauchy-Schwarz inequality allows us to derive

$$I_2 = \left| \sum_{k=K+1}^{\infty} e^{-\mu_k t} \psi_k(x_i) \psi_k(x_j) \right| \leq \sup_{x \in \mathcal{M}} \sum_{k=K+1}^{\infty} e^{-\mu_k t} |\psi_k(x)|^2.$$

Utilizing techniques akin to those detailed by [4] (on page 393), the right-hand side of the above inequality can be bounded by the following integral

$$\sup_{x \in \mathcal{M}} \sum_{k=K+1}^{\infty} e^{-\mu_k t} |\psi_k(x)|^2 \leq D_2 t^{-\frac{d}{2}} \int_{t\mu_{K+1}}^{\infty} s^{\frac{d}{2}} e^{-s} ds,$$

where D_2 is an absolute constant that depends solely on \mathcal{M} . Combined with (2.6), we have

$$I_2 \leq D_2 t^{-\frac{d}{2}} \int_{C_{low}(K+1) \frac{2}{d} t}^{\infty} s^{\frac{d}{2}} e^{-s} ds. \quad (\text{B.1})$$

It is noteworthy that

$$\Gamma(a, x) = \int_x^{\infty} s^{a-1} e^{-s} ds$$

represents the incomplete Gamma function. According to [6], we obtain the following estimation:

$$|\Gamma(a, x)| \leq x^{a-1} e^{-x} \cdot \frac{c}{c-1},$$

which holds for any $c > 1, a \geq 1$ and $|x| \geq c(a-1)$. Returning to our estimation (B.1), if we set $c = 2$, then whenever $C_{low}(K+1)^{\frac{2}{d}} t \geq d$, or equivalently,

$$K \geq \left(\frac{d}{C_{low} t} \right)^{\frac{d}{2}} - 1,$$

we can deduce an upper bound for I_2 as:

$$\begin{aligned} I_2 &\leq D_2 t^{-\frac{d}{2}} \cdot 2 \left(C_{low}(K+1)^{\frac{2}{d}} t \right)^{\frac{d}{2}} e^{-C_{low}(K+1)^{\frac{2}{d}} t} \\ &\leq 2D_2 C_{low}^{\frac{d}{2}} (K+1) e^{-C_{low}(K+1)^{\frac{2}{d}} t}. \end{aligned} \quad (\text{B.2})$$

Now we return to I_1 . We further decompose it as

$$\begin{aligned} \left| \sum_{k=1}^K (e^{-\tilde{\mu}_k t} \tilde{v}_k(i) \tilde{v}_k(j) - e^{-\mu_k t} \psi_k(x_i) \psi_k(x_j)) \right| &\leq \left| \sum_{k=1}^K (e^{-\tilde{\mu}_k t} - e^{-\mu_k t}) \psi_k(x_i) \psi_k(x_j) \right| \\ &\quad + \left| \sum_{k=1}^K (\tilde{v}_k(i) \tilde{v}_k(j) - \psi_k(x_i) \psi_k(x_j)) e^{-\tilde{\mu}_k t} \right|. \end{aligned}$$

For the first term in the aforementioned inequality, by applying (2.35) we obtain

$$\begin{aligned} |e^{-\tilde{\mu}_k t} - e^{-\mu_k t}| &\leq e^{-\mu_k t} |e^{-(\tilde{\mu}_k - \mu_k)t} - 1| \\ &\leq e^{-\mu_k t} |\tilde{\mu}_k - \mu_k| t \\ &\leq C_1 \epsilon t e^{-\mu_1 t} \leq C_1 \epsilon t. \end{aligned}$$

Here, ϵ serves as shorthand notation for $\left(\frac{\log N}{N} \right)^{\frac{1}{\frac{d}{2}+2}}$, consistent with the parameterization used in Theorem 1. Combining with (2.7) we have

$$\begin{aligned} \left| \sum_{k=1}^K (e^{-\tilde{\mu}_k t} - e^{-\mu_k t}) \psi_k(x_i) \psi_k(x_j) \right| &\leq \sum_{k=1}^K C_1 \epsilon t D_1^2 \mu_k^{\frac{d-1}{2}} \\ &\leq D_1^2 C_1 \epsilon t K \mu_K^{\frac{d-1}{2}}. \end{aligned} \quad (\text{B.3})$$

For the second term, for any $1 \leq k \leq K$, the combination of (2.36) with (2.7) yields:

$$\begin{aligned} |\tilde{v}_k(i) \tilde{v}_k(j) - \psi_k(x_i) \psi_k(x_j)| &\leq |\tilde{v}_k(i) (\tilde{v}_k(j) - \psi_k(x_j)) + \psi_k(x_j) (\tilde{v}_k(i) - \psi_k(x_i))| \\ &\leq \max_{1 \leq i \leq N} |\tilde{v}_k(i) - \psi_k(x_i)| \cdot \left(\max_{1 \leq i \leq N} |\tilde{v}_k(i)| + \max_{1 \leq i \leq N} |\psi_k(x_i)| \right) \\ &\leq C_2 \sqrt{\epsilon} \cdot \left(\max_{1 \leq i \leq N} |\tilde{v}_k(i) - \psi_k(x_i)| + 2 \max_{1 \leq i \leq N} |\psi_k(x_i)| \right) \\ &\leq C_2 \sqrt{\epsilon} \cdot \left(C_2 \sqrt{\epsilon} + 2D_1 \mu_k^{\frac{d-1}{4}} \right) \\ &\leq 3C_2 D_1 \mu_k^{\frac{d-1}{4}} \sqrt{\epsilon}. \end{aligned}$$

The last inequality in this formulation is derived under the condition that $\epsilon \ll 1$. Given that $|\tilde{\mu}_k - \mu_k| \leq C_1 \epsilon \leq \frac{1}{2} \mu_k$ for $2 \leq k \leq K$ and $\tilde{\mu}_1 = \mu_1 = 0$, we can deduce

$$|e^{-\tilde{\mu}_k t}| \leq |e^{-\frac{1}{2} \mu_k t}| \leq |e^{-\frac{1}{2} \mu_1 t}| \leq 1,$$

which is valid for all $1 \leq k \leq K$. Consequently, we obtain

$$\left| \sum_{k=1}^K (\tilde{v}_k(i) \tilde{v}_k(j) - \psi_k(x_i) \psi_k(x_j)) e^{-\tilde{\mu}_k t} \right| \leq 3C_2 D_1 K \mu_k^{\frac{d-1}{4}} \sqrt{\epsilon}. \quad (\text{B.4})$$

By combining (B.3) and (B.4) we have

$$\begin{aligned} I_1 &\leq D_1^2 C_1 t \epsilon K \mu_K^{\frac{d-1}{2}} + 3C_2 D_1 K \mu_k^{\frac{d-1}{4}} \sqrt{\epsilon} \\ &\leq 4D_1^2 C_1 C_2 t \sqrt{\epsilon} K \mu_K^{\frac{d-1}{2}}. \end{aligned} \quad (\text{B.5})$$

Finally, by integrating the upper bounds (B.5) and (B.2) we ascertain that

$$\left| H_t(x_i, x_j) - \tilde{H}_{t,K}(i, j) \right| \leq 4D_1^2 C_1 C_2 t \sqrt{\epsilon} K \mu_K^{\frac{d-1}{2}} + 2D_2 C_{low}^{\frac{d}{2}} (K+1) e^{-C_{low}(K+1)^{\frac{2}{d}} t}.$$

Therefore, given our selection of K, ϵ , which adhere to the conditions

$$(K+1) e^{-C_{low}(K+1)^{\frac{2}{d}} t} \leq \frac{1}{K},$$

$$\epsilon^{\frac{1}{4}} \leq \frac{1}{C_1 C_2 K \mu_K^{\frac{d-1}{2}}},$$

we ultimately attain the desired upper bound

$$\left| H_t(x_i, x_j) - \tilde{H}_{t,K}(i, j) \right| \leq 4D_1^2 t \epsilon^{\frac{1}{4}} + 2D_2 C_{low}^{\frac{d}{2}} \frac{1}{K}.$$

This completes the proof. \square

C Proof of Theorem 3

Proof. Drawing on the classical Weyl's perturbation inequality, as discussed in [61, 27], we obtain for any $1 \leq k \leq m$,

$$|\tilde{\lambda}_k - \hat{\lambda}_k| \leq \|\tilde{H}_{t,m} - H_t\|_2, \quad (\text{C.1})$$

where $\|\cdot\|_2$ denotes the operator 2-norm. Let $\boldsymbol{\varepsilon} = \tilde{H}_{t,m} - H_t$ represent an $m \times m$ matrix with entries:

$$|\boldsymbol{\varepsilon}_{ij}| \leq \frac{1}{m} \left(\frac{C_a}{K} + C_b \epsilon^{\frac{1}{4}} \right)$$

derived from (3.1). Given that $\|\boldsymbol{\varepsilon}\|_2 = \max\{x^T \boldsymbol{\varepsilon} y : \|x\|_2 = \|y\|_2 = 1\}$, it follows that

$$\|\boldsymbol{\varepsilon}\|_2 = x^T \boldsymbol{\varepsilon} y \leq \sup_{i,j} |\boldsymbol{\varepsilon}_{ij}| \cdot \sum_{i,j=1}^m |x_i y_j| \leq \sup_{i,j} |\boldsymbol{\varepsilon}_{ij}| \cdot m \leq \frac{C_a}{K} + C_b \epsilon^{\frac{1}{4}}. \quad (\text{C.2})$$

This insight, when integrated with (C.1), facilitates the derivation of the desired eigenvalue estimation (3.3). Progressing to eigenvector estimations, Davis-Kahan's theorem, which is often referred to as the $\sin \theta$ theorem, as discussed in [21, 46], allows for a comparison between the eigen-pairs $(\tilde{\lambda}_k, \tilde{u}_k)$ of the matrix $\tilde{H}_{t,m}$ and a corresponding unit eigenvector \hat{u}_k of the matrix H_t , associated with the eigenvalue $\hat{\lambda}_k$, leading to the relationship

$$|\sin \langle \tilde{u}_k, \hat{u}_k \rangle| \leq \frac{\|\varepsilon\|_2}{\delta_k}.$$

Here, $\langle \tilde{u}_k, \hat{u}_k \rangle$ signifies the angle between \tilde{u}_k and \hat{u}_k , and δ_k represents the eigen-gap of H_t with respect to the eigenvalue $\hat{\lambda}_k$, defined as $\delta_k = \min\{|\hat{\lambda}_j - \hat{\lambda}_k| : \hat{\lambda}_j \neq \hat{\lambda}_k\}$. Given that:

$$\|\tilde{u}_k - \hat{u}_k\|_\infty \leq \|\tilde{u}_k - \hat{u}_k\|_2 \leq |\langle \tilde{u}_k, \hat{u}_k \rangle| \leq \frac{\pi}{2} |\sin \langle \tilde{u}_k, \hat{u}_k \rangle|,$$

where the second inequality is derived from the geometric principle that an arc's length on a unit circle is always greater than the length of its chord. Consequently, this leads to the relationship

$$\|\tilde{u}_k - \hat{u}_k\|_\infty \leq \frac{\pi \|\varepsilon\|_2}{2 \delta_k}. \quad (\text{C.3})$$

To establish a lower bound for the eigen-gap δ_k , it's pivotal to consider that the matrix H_t represents the heat kernel matrix with entries $\frac{1}{m} H_t(x_i, x_j)$. The integral operator of the heat kernel on $L^2(\nu)$ is L_ν , which can be expressed through spectral decomposition (2.16). According to [39, 7], for any $1 \leq k \leq m$, and for a fixed integer $1 \leq l \leq m$, with a probability of at least $1 - 2e^{-\tau}$, it holds

$$|\hat{\lambda}_k - pe^{-\mu_k t}| = O\left(pe^{-\mu_k t}(pe^{-\mu_1 t})^{-\frac{1}{2}} l^2 m^{-\frac{1}{2}} + \Lambda_{>l} + \sqrt{\Lambda_{>l} m^{-\frac{1}{2}}}\right), \quad (\text{C.4})$$

where $\Lambda_{>l} = \sum_{j=l+1}^{\infty} pe^{-\mu_j t}$. Setting $l = \left(\frac{\log m}{3C_{low} t}\right)^{\frac{d}{2}}$, we can derive

$$\begin{aligned} \Lambda_{>l} &= \sum_{j=l+1}^{\infty} pe^{-\mu_j t} \leq \sum_{j=l+1}^{\infty} pe^{-C_{low} t j^{\frac{2}{d}}} \\ &\lesssim \int_{l+1}^{\infty} e^{-C_{low} t x^{\frac{2}{d}}} dx \\ &\lesssim \int_{C_{low} t l^{\frac{2}{d}+1}}^{\infty} u^{\frac{d}{2}-1} e^{-u} du \\ &\lesssim (C_{low} t l^{\frac{2}{d}+1})^{\frac{d}{2}-1} e^{-(C_{low} t l^{\frac{2}{d}+1})} \\ &\lesssim l e^{-C_{low} t l^{\frac{2}{d}}} \\ &\lesssim (\log m)^{\frac{d}{2}} m^{-\frac{1}{3}}. \end{aligned} \quad (\text{C.5})$$

The fourth inequality above again emerges from the estimation involving the incomplete Gamma function as in the Appendix B. Consequently, this leads to the establishment of

$$\sqrt{\Lambda_{>l} m^{-\frac{1}{2}}} \lesssim \sqrt{(\log m)^{\frac{d}{2}} m^{-\frac{1}{3}} m^{-\frac{1}{2}}} \lesssim (\log m)^{\frac{d}{4}} m^{-\frac{2}{3}}.$$

Notice that $\mu_k \geq \mu_1 = 0$, we have

$$\begin{aligned} pe^{-\mu_k t} (pe^{-\mu_1 t})^{-\frac{1}{2}} l^2 m^{-\frac{1}{2}} &\lesssim \left(e^{-C_{low} t l^{\frac{2}{d}}} \right)^{-\frac{1}{2}} l^2 m^{-\frac{1}{2}} \\ &\lesssim m^{\frac{1}{6}} (\log m)^d m^{-\frac{1}{2}} \\ &\lesssim (\log m)^d m^{-\frac{1}{3}}. \end{aligned}$$

By integrating these estimations into (C.4), we ascertain that, for any $1 \leq k \leq m$,

$$|\hat{\lambda}_k - pe^{-\mu_k t}| = O\left((\log m)^d m^{-\frac{1}{3}}\right). \quad (\text{C.6})$$

For any $1 \leq k \leq q$, there exists some j (dependent on k) such that

$$\begin{aligned} \delta_k &= |\hat{\lambda}_j - \hat{\lambda}_k| \\ &\geq |pe^{-\mu_j t} - pe^{-\mu_k t}| - O\left((\log m)^d m^{-\frac{1}{3}}\right) \\ &= pe^{-\mu_k t} |1 - e^{(\mu_k - \mu_j)t}| - O\left((\log m)^d m^{-\frac{1}{3}}\right) \\ &\geq pe^{-\mu_k t} t |\mu_k - \mu_j| - O\left((\log m)^d m^{-\frac{1}{3}}\right) \\ &\geq pe^{-\mu_q t} t \gamma_q - O\left((\log m)^d m^{-\frac{1}{3}}\right), \end{aligned}$$

where $\gamma_q = \min\{|\mu_j - \mu_k| : \mu_j \neq \mu_k, 1 \leq j, k \leq q\}$ represents the smallest eigen-gap among the first q eigenvalues of the Laplacian Δ . Given the asymptotic behavior $\mu_k \sim k^{\frac{2}{d}}$ as $k \rightarrow \infty$, it follows that the eigen-gap between μ_k and μ_{k+1} also increases to infinite. Consequently, as $q \sim (\log m)^{\frac{d}{2}} \rightarrow \infty$, γ_q becomes a constant not dependent on m . Furthermore, given that $r > 1$, (3.2) yields

$$\begin{aligned} \delta_k &\geq pe^{-C_{up} t q^{\frac{2}{d}}} t \gamma_q - O\left((\log m)^d m^{-\frac{1}{3}}\right) \\ &\geq pt \gamma_q m^{-\frac{1}{2r+1}} - O\left((\log m)^d m^{-\frac{1}{3}}\right) \\ &\gtrsim m^{-\frac{1}{2r+1}}. \end{aligned} \quad (\text{C.7})$$

Finally, combining (C.2), (C.3), and (C.7) yields

$$\|\tilde{u}_k - \hat{u}_k\|_{\infty} \lesssim m^{\frac{1}{2r+1}} \left(\frac{1}{K} + \epsilon^{\frac{1}{4}} \right),$$

which is the desired result. The proof is then finished. \square

D Proof of Lemma 2

Proof. For any $1 \leq k \leq q$ and any $1 \leq j \leq N$ we have

$$\begin{aligned}
|\phi_k(x_j) - \tilde{\phi}_k(j)| &= \left| \frac{1}{\sqrt{m\hat{\lambda}_k}} \sum_{i=1}^m \hat{u}_k(i) H_t(x_i, x_j) - \frac{1}{\sqrt{m\tilde{\lambda}_k}} \sum_{i=1}^m \tilde{u}_k(i) \tilde{H}_{t,K}(i, j) \right| \\
&\leq \frac{1}{\sqrt{m\hat{\lambda}_k}} \left| \sum_{i=1}^m \hat{u}_k(i) H_t(x_i, x_j) - \sum_{i=1}^m \tilde{u}_k(i) \tilde{H}_{t,K}(i, j) \right| \\
&\quad + \left| \frac{1}{\sqrt{m\hat{\lambda}_k}} - \frac{1}{\sqrt{m\tilde{\lambda}_k}} \right| \cdot \left| \sum_{i=1}^m \tilde{u}_k(i) \tilde{H}_{t,K}(i, j) \right| \\
&\triangleq I_1 + I_2.
\end{aligned}$$

Addressing I_1 , (C.6) yields

$$\begin{aligned}
\hat{\lambda}_k &\geq pe^{-\mu_k t} - O\left((\log m)^d m^{-\frac{1}{3}}\right) \\
&\geq pe^{-\mu_q t} - O\left((\log m)^d m^{-\frac{1}{3}}\right) \\
&\gtrsim m^{-\frac{1}{2r+1}} - O\left((\log m)^d m^{-\frac{1}{3}}\right) \\
&\gtrsim m^{-\frac{1}{2r+1}}.
\end{aligned} \tag{D.1}$$

This leads us to conclude that:

$$\frac{1}{\sqrt{m\hat{\lambda}_k}} \lesssim m^{-\frac{r}{2r+1}}. \tag{D.2}$$

Furthermore, by leveraging (2.39) and (3.4) we obtain

$$\begin{aligned}
\left| \sum_{i=1}^m \hat{u}_k(i) H_t(x_i, x_j) - \sum_{i=1}^m \tilde{u}_k(i) \tilde{H}_{t,K}(i, j) \right| &\leq \left| \sum_{i=1}^m (\hat{u}_k(i) - \tilde{u}_k(i)) H_t(x_i, x_j) \right| \\
&\quad + \left| \sum_{i=1}^m \tilde{u}_k(i) (H_t(x_i, x_j) - \tilde{H}_{t,K}(i, j)) \right| \\
&\leq m\kappa^2 C_c m^{\frac{1}{2r+1}} \left(\frac{1}{K} + \epsilon^{\frac{1}{4}} \right) + m \left(\frac{C_a}{K} + C_b \epsilon^{\frac{1}{4}} \right) \\
&\lesssim m^{1+\frac{1}{2r+1}} \left(\frac{1}{K} + \epsilon^{\frac{1}{4}} \right),
\end{aligned}$$

where the second inequality in this calculation is a result of the boundedness of H_t and the unit vector property of \tilde{u}_k . Consequently, we arrive at the following bound:

$$I_1 \lesssim m^{\frac{r+2}{2r+1}} \left(\frac{1}{K} + \epsilon^{\frac{1}{4}} \right). \tag{D.3}$$

For bounding I_2 , a similar approach yields

$$\begin{aligned}
\left| \sum_{i=1}^m \tilde{u}_k(i) \tilde{H}_{t,K}(i, j) \right| &\leq \sum_{i=1}^m \left| \tilde{H}_{t,K}(i, j) \right| \\
&\leq \sum_{i=1}^m \left| \tilde{H}_{t,K}(i, j) - H_t(x_i, x_j) \right| + \sum_{i=1}^m |H_t(x_i, x_j)| \\
&\leq m \left(\frac{C_a}{K} + C_b \epsilon^{\frac{1}{4}} \right) + m \kappa^2 \lesssim m.
\end{aligned}$$

Additionally, we have

$$\begin{aligned}
\left| \frac{1}{\sqrt{m \hat{\lambda}_k}} - \frac{1}{\sqrt{m \tilde{\lambda}_k}} \right| &= m^{-\frac{1}{2}} \left| \frac{1}{\sqrt{\hat{\lambda}_k}} - \frac{1}{\sqrt{\tilde{\lambda}_k}} \right| \\
&= m^{-\frac{1}{2}} \left| \frac{\sqrt{\tilde{\lambda}_k} - \sqrt{\hat{\lambda}_k}}{\sqrt{\hat{\lambda}_k} \sqrt{\tilde{\lambda}_k}} \right| \\
&= m^{-\frac{1}{2}} \left| \frac{\tilde{\lambda}_k - \hat{\lambda}_k}{\sqrt{\hat{\lambda}_k} \sqrt{\tilde{\lambda}_k} (\sqrt{\tilde{\lambda}_k} + \sqrt{\hat{\lambda}_k})} \right|.
\end{aligned}$$

Drawing from (3.3) and (D.1), we obtain

$$\tilde{\lambda}_k \gtrsim m^{-\frac{1}{2r+1}} - \left(\frac{C_a}{K} + C_b \epsilon^{\frac{1}{4}} \right) \gtrsim m^{-\frac{1}{2r+1}}, \tag{D.4}$$

and hence

$$\left| \frac{1}{\sqrt{m \hat{\lambda}_k}} - \frac{1}{\sqrt{m \tilde{\lambda}_k}} \right| \lesssim m^{-\frac{1}{2}} m^{\frac{3}{2} \cdot \frac{1}{2r+1}} \left(\frac{C_a}{K} + C_b \epsilon^{\frac{1}{4}} \right).$$

This leads us to conclude

$$I_2 \lesssim m^{\frac{1}{2} + \frac{3}{2} \cdot \frac{1}{2r+1}} \left(\frac{1}{K} + \epsilon^{\frac{1}{4}} \right) \lesssim m^{\frac{r+2}{2r+1}} \left(\frac{1}{K} + \epsilon^{\frac{1}{4}} \right). \tag{D.5}$$

Finally, by merging (D.3) and (D.5), we achieve the desired result

$$|\phi_k(x_j) - \tilde{\phi}_k(j)| \lesssim m^{\frac{r+2}{2r+1}} \left(\frac{1}{K} + \epsilon^{\frac{1}{4}} \right).$$

The proof is then finished. \square

E Complementary Discussions of Proof for Lemma 4

E.1 Modification of Lemma 10 in [62]

In this section, we present a detailed proof for the assertion mentioned as (5.14). It is important to note that, in the groundwork laid out for Lemma 10 in [62], the majority of

supplementary lemmas are readily adaptable to a scenario where $\beta = 2$, with only one exception, the Lemma 8. Consequently, our primary focus will be on expanding the scope of Lemma 8 in [62] to incorporate $\beta = 2$. In other words, we aim to establish the following result:

$$\left\| (T_\delta + \lambda I)^{\frac{1}{2}} h_\lambda(T_\delta) f_{P,\lambda} \right\|_{\mathcal{H}_t} \lesssim \lambda. \quad (\text{E.1})$$

Notice that

$$\left\| (T_\delta + \lambda I)^{\frac{1}{2}} h_\lambda(T_\delta) f_{P,\lambda} \right\|_{\mathcal{H}_t} = \left\| (T_\delta + \lambda I)^{\frac{1}{2}} h_\lambda(T_\delta) g_\lambda(T_\nu) I_\nu^* f^* \right\|_{\mathcal{H}_t}.$$

Since Assumption 1 implies that $f \in \mathcal{H}_t$, there exists another function $g_0 \in L^2(\nu)$ such that $f^* = L_\nu g_0$. Consequently,

$$\begin{aligned} \left\| (T_\delta + \lambda I)^{\frac{1}{2}} h_\lambda(T_\delta) f_{P,\lambda} \right\|_{\mathcal{H}_t} &= \left\| (T_\delta + \lambda I)^{\frac{1}{2}} h_\lambda(T_\delta) g_\lambda(T_\nu) I_\nu^* L_\nu g_0 \right\|_{\mathcal{H}_t} \\ &= \left\| (T_\delta + \lambda I)^{\frac{1}{2}} h_\lambda(T_\delta) g_\lambda(T_\nu) T_\nu I_\nu^* g_0 \right\|_{\mathcal{H}_t} \\ &\leq \left\| (T_\delta + \lambda I)^{\frac{1}{2}} h_\lambda(T_\delta) g_\lambda(T_\nu) T_\nu I_\nu^* \right\|_{\mathcal{B}(L^2, \mathcal{H}_t)} \cdot \|g_0\|_{L^2(\nu)} \\ &= \left\| (T_\delta + \lambda I)^{\frac{1}{2}} h_\lambda(T_\delta) g_\lambda(T_\nu) T_\nu T_\nu^{\frac{1}{2}} \right\|_{\mathcal{B}(\mathcal{H}_t)} \cdot \|g_0\|_{L^2(\nu)}, \end{aligned}$$

where the last equation follows from the fact that I_ν^* and $T_\nu^{\frac{1}{2}}$ are self-adjoint operators with same eigen-system. Then we further decompose the above expression as

$$\begin{aligned} \left\| (T_\delta + \lambda I)^{\frac{1}{2}} h_\lambda(T_\delta) g_\lambda(T_\nu) T_\nu T_\nu^{\frac{1}{2}} \right\|_{\mathcal{B}(\mathcal{H}_t)} &\leq \left\| (T_\delta + \lambda I)^{\frac{1}{2}} h_\lambda(T_\delta) (T_\delta + \lambda I)^{\frac{1}{2}} \right\|_{\mathcal{B}(\mathcal{H}_t)} \\ &\quad \cdot \left\| (T_\delta + \lambda I)^{-\frac{1}{2}} (T_\nu + \lambda I)^{\frac{1}{2}} \right\|_{\mathcal{B}(\mathcal{H}_t)} \\ &\quad \cdot \left\| (T_\nu + \lambda I)^{-\frac{1}{2}} T_\nu^{\frac{1}{2}} \right\|_{\mathcal{B}(\mathcal{H}_t)} \cdot \|g_\lambda(T_\nu) T_\nu\|_{\mathcal{B}(\mathcal{H}_t)}. \end{aligned}$$

From (5.18) and (5.6) we have

$$\left\| (T_\delta + \lambda I)^{\frac{1}{2}} h_\lambda(T_\delta) (T_\delta + \lambda I)^{\frac{1}{2}} \right\|_{\mathcal{B}(\mathcal{H}_t)} = \|(T_\delta + \lambda I) h_\lambda(T_\delta)\|_{\mathcal{B}(\mathcal{H}_t)} \leq 2\lambda,$$

and

$$\left\| (T_\delta + \lambda I)^{-\frac{1}{2}} (T_\nu + \lambda I)^{\frac{1}{2}} \right\|_{\mathcal{B}(\mathcal{H}_t)} \leq \sqrt{3}.$$

By a direct calculation, we derive that

$$\left\| (T_\nu + \lambda I)^{-\frac{1}{2}} T_\nu^{\frac{1}{2}} \right\|_{\mathcal{B}(\mathcal{H}_t)} = \sup_{k \in \mathbb{N}} \left(\frac{e^{-\mu_k t}}{e^{-\mu_k t} + \lambda} \right)^{\frac{1}{2}} \leq 1.$$

Finally, property (2.25) yields

$$\|g_\lambda(T_\nu) T_\nu\|_{\mathcal{B}(\mathcal{H}_t)} \leq 1.$$

Our targeted (E.1) then follows from above pieces. The proof is then finished. \square

E.2 Modification of Theorem 1 in [62]

In this section, we extend the original proof in [62] for Theorem 1 to our setting with $\beta = 2$ in details. We begin with (5.14):

$$\left\| (T_\nu + \lambda I)^{-\frac{1}{2}} (g_D - T_\delta f_{P,\lambda}) \right\|_{\mathcal{H}_t}^2 \lesssim \frac{1}{m} \left(N_\nu(\lambda) + \lambda^{2-\alpha} + \frac{L_\lambda^2}{m\lambda^\alpha} \right) + \lambda^2.$$

From Lemma 4 in [62], it holds

$$N_\nu(\lambda) \lesssim (\log \lambda^{-1})^{\frac{d}{2}}.$$

Since

$$\lambda \sim \left(\frac{(\log m)^{\frac{d}{2}}}{m} \right)^{\frac{1}{2}},$$

we have $\lambda \rightarrow 0$ as $m \rightarrow \infty$. Therefore,

$$N_\nu(\lambda) + \lambda^{2-\alpha} \lesssim (\log \lambda^{-1})^{\frac{d}{2}}.$$

For the third term in the bracket, we have

$$\frac{L_\lambda^2}{m\lambda^\alpha} = \frac{1}{m\lambda^\alpha} \cdot \max\{M, \|f_{P,\lambda} - f^*\|_\infty\}.$$

Exploiting Lemma 1 in [62] with $\gamma = \alpha$, $\beta = 2$ combining with the embedding property $\mathcal{H}_t^\alpha \hookrightarrow L^\infty(\nu)$, we derive that

$$\|f_{P,\lambda} - f^*\|_\infty \lesssim \lambda^{2-\alpha}.$$

Hence

$$\frac{L_\lambda^2}{m\lambda^\alpha} \lesssim \frac{1}{m\lambda^\alpha},$$

which also tends to 0 as $m \rightarrow \infty$. Therefore,

$$\left\| (T_\nu + \lambda I)^{-\frac{1}{2}} (g_D - T_\delta f_{P,\lambda}) \right\|_{\mathcal{H}_t}^2 \lesssim \frac{1}{m} (\log \lambda^{-1})^{\frac{d}{2}} + \lambda^2.$$

A direct calculation shows

$$\frac{1}{m} (\log \lambda^{-1})^{\frac{d}{2}} \sim \frac{\left(\frac{1}{2}(\log m - \frac{d}{2} \log \log m)\right)^{\frac{d}{2}}}{m} \lesssim \frac{(\log m)^{\frac{d}{2}}}{m}.$$

Combining with the fact that

$$\lambda^2 \sim \frac{(\log m)^{\frac{d}{2}}}{m},$$

we finally derive

$$\left\| (T_\nu + \lambda I)^{-\frac{1}{2}} (g_D - T_\delta f_{P,\lambda}) \right\|_{\mathcal{H}_t}^2 \lesssim \frac{(\log m)^{\frac{d}{2}}}{m} \sim \lambda^2. \quad (\text{E.2})$$

The upper bound delineated in (E.2) is exactly (5.15), which forms the essence of the proof for Theorem 1 in [62]. Specifically, the synergy between (E.2) and (E.1), when integrated with the integral operator techniques adopted in Section 5, supports the *estimation* error analysis, while the original *approximation* error analysis can be extended to $\beta = 2$ directly. Therefore, our proof ends with the same approach as in [62]. The proof is then finished. \square

F Convergence Rate for Tikhonov Regularization

Before the detailed proof of the convergence rate for Tikhonov regularization, we note that with $g_\lambda(t) = \frac{1}{\lambda+t}$, this filter function exhibits Lipschitz continuity, characterized by a Lipschitz constant of λ^{-2} . This continuity property provides a solid foundation for establishing enhanced convergence results, particularly for the term I_1 as discussed in Lemma 6. Specifically, we have

$$\begin{aligned} I_1 &= \left| \sum_{k=1}^q \left(g_\lambda(\lambda_k) - g_\lambda(\tilde{\lambda}_k) \right) \langle g_D, \phi_k \rangle_{\mathcal{H}_t} \phi_k(x_j) \right| \\ &\leq \sum_{k=1}^q \left| g_\lambda(\lambda_k) - g_\lambda(\tilde{\lambda}_k) \right| \cdot |\langle g_D, \phi_k \rangle_{\mathcal{H}_t}| \cdot |\phi_k(x_j)|. \end{aligned}$$

By Lipschitz property of g_λ , we have

$$\left| g_\lambda(\lambda_k) - g_\lambda(\tilde{\lambda}_k) \right| \leq \lambda^{-2} |\lambda_k - \tilde{\lambda}_k| \lesssim \lambda^{-2} \left(\frac{1}{K} + \epsilon^{\frac{1}{4}} \right),$$

and the remaining term of I_1 are already bounded in (5.25) and (5.23). Combining these pieces yields

$$\begin{aligned} I_1 &\lesssim q \cdot \lambda^{-2} \left(\frac{1}{K} + \epsilon^{\frac{1}{4}} \right) \cdot m^{\frac{r+1}{2r+1}} \\ &\lesssim m^{\frac{r+1}{2r+1}+1} \cdot \left(\frac{1}{K} + \epsilon^{\frac{1}{4}} \right). \end{aligned}$$

Using this improved upper bound for I_1 , we can then enhance the overall convergence rate for Tikhonov regularization to become

$$|\tilde{f}_{D,\lambda}(j) - f^*(x_j)| \lesssim m^{-\frac{C_{low}}{C_{up}} \cdot \frac{1}{2} + \frac{\alpha}{4}} (\log m)^{\frac{1}{2} + \frac{d}{4} - \frac{\alpha d}{8}} + m^{\frac{\max\{3, r+1\}}{2r+1} + 1} (\log m)^{\frac{d}{2}} \cdot \left(\frac{1}{K} + \epsilon^{\frac{1}{4}} \right).$$

Therefore, a similar approach as in section 3.2 will give the desired convergence rate (3.14). This completes the proof. \square